

TECHNISCHE UNIVERSITÄT MÜNCHEN

Lehrstuhl für Grünlandlehre

The Turnover of Respiratory Carbon Pools in Grass Plants –
Assessment by Dynamic ^{13}C Labeling and Compartmental Analysis of
Tracer Kinetics in Respired CO_2

Christoph Andreas Lehmeier

Vollständiger Abdruck der von der Fakultät Wissenschaftszentrum Weihenstephan für Ernährung, Landnutzung und Umwelt der Technischen Universität München zur Erlangung des akademischen Grades eines

Doktors der Agrarwissenschaften
genehmigten Dissertation.

Vorsitzender: Univ.-Prof. Dr. U. Schmidhalter

Prüfer der Dissertation: 1. Univ.-Prof. Dr. H. Schnyder
2. Univ.-Prof. Dr. R. Matyssek

Die Dissertation wurde am 13.10.2008 bei der Technischen Universität München eingereicht und durch die Fakultät Wissenschaftszentrum Weihenstephan für Ernährung, Landnutzung und Umwelt am 10.11.2008 angenommen.

Contents

Contents	ii
Abstract	iii
Zusammenfassung	v
List of Figures	vii
List of Tables	ix
Chapter I: General Introduction	1
Chapter II: Root and Shoot Respiration of Perennial Ryegrass Are Supplied by the Same Substrate Pools: Assessment by Dynamic ^{13}C Labeling and Compartmental Analysis of Tracer Kinetics	5
Chapter III: Nitrogen Deficiency Increases the Residence Time of Carbon in the Respiratory Supply System of Perennial Ryegrass and Reveals a Constitutive Role of Long-term Stores	27
Chapter IV: General and Summarizing Discussion	47
References	54
Lebenslauf	60

Abstract

Aims: The subject of the present thesis was the functional identification of the substrate pools forming the respiratory carbon supply system of perennial ryegrass (*Lolium perenne* L.). Of particular interest was (i) to determine their size, turnover rates and their contributions to carbon release in respiration of shoots and roots of intact plants, and (ii) to explore the effects of plants' nitrogen supply level on substrate pool properties.

Materials and Methods: Stands of perennial ryegrass were grown in controlled environments with continuous light and a contrasting level of nitrate supply by otherwise identical and constant growth conditions. Individual plants were labeled with $^{13}\text{CO}_2/^{12}\text{CO}_2$ for periods ranging from 1 h to 1 month, followed by measurements of the $^{13}\text{C}/^{12}\text{C}$ ratios of shoot- and root-respired CO_2 in the dark. The time courses of tracer incorporation into respired CO_2 were analyzed with compartmental models, a mathematical tool which helped to extract information about the number and characteristics of the substrate pools supplying carbon to respiration.

Results and Discussion: Compartmental analysis of CO_2 respired by plants grown in high nitrogen supply level revealed that 95% of shoot and root respiration was supplied by three substrate pools which differed greatly in their rates of turnover. A very slow pool whose kinetics could not be characterized provided the remaining 5%. Two small, rapidly turned over pools of current assimilate provided almost half of respired carbon, while the other half was supplied by a big short-term store with slower turnover. This was true for both shoots and roots, and from this and further evidence, we argue that shoot and root respiration was supplied by the same substrate pools. The same model explained the time course of tracer incorporation into CO_2 respired by plants grown in nitrogen limited conditions equally well. The size of the respiratory supply system, however, increased by 30% with nitrogen limitation, and half-lives were, at least in part, dramatically increased. Long-term stores became a substantial carbon source, and this resulted in a longer mean residence time of carbon in the respiratory supply system: from 36 h in full nitrogen supply to almost 6 d under nitrogen limited conditions.

Conclusions: This work presents for the first time a conceptual model of the respiratory carbon supply system of perennial ryegrass which was based on empirical evidence, and it revealed a tight plant-level integration of respiratory carbon pools and fluxes. The model was proved to be valid for a range of external nitrogen availability, even though substrate pool properties showed pronounced responses to the level of nitrogen supply. The residence time

of carbon in the respiratory supply system was closely linked to plants' nitrogen status and mainly controlled *via* current photosynthate and deposition/mobilization fluxes involving either short-term storage (in high nitrogen supply) or long-term storage (in low nitrogen supply) components. The major part of the respiratory carbon was located in above-ground biomass, which placed the shoot in the position of controlling carbon allocation within the respiratory supply system.

Zusammenfassung

Zielsetzung: Die vorliegende Arbeit befasst sich mit der Identifizierung der funktionellen Eigenschaften jener Substratpools, die das Kohlenstoff-Versorgungssystem der Respiration von Deutsch Weidelgras (*Lolium perenne* L.) darstellen. Insbesondere sollte sowohl deren Größe und Umsetzungsrate erfasst als auch ihre quantitative Bedeutung als Kohlenstoffquelle für die Respiration von Spross und Wurzel von intakten Pflanzen bestimmt werden. Ein weiteres Augenmerk lag auf den möglichen Auswirkungen des Stickstoffversorgungsniveaus der Pflanzen auf die Eigenschaften der respiratorischen Substratpools.

Material und Methoden: Pflanzenbestände von Deutsch Weidelgras wurden in kontrastierenden Stickstoffversorgungsniveaus im Dauerlicht unter kontrollierten Bedingungen angezogen. Einzelne, zufällig ausgewählte Pflanzen wurden mit $^{13}\text{CO}_2/^{12}\text{CO}_2$ für Zeiträume von 1 h bis 1 Monat isotopisch markiert; am Ende der Markierungszeiträume wurden die Respirationsraten von Spross und Wurzel sowie die Isotopensignatur des respirierten CO_2 im Dunkeln gemessen. Die Erscheinungsraten von markiertem Kohlenstoff im respirierten CO_2 wurden einer kompartmentellen Analyse unterzogen; dies ist eine mathematische Vorgehensweise, um Informationen über Anzahl und Eigenschaften jener Substratpools zu erhalten, die an der Kohlenstoffversorgung der Respiration beteiligt sind.

Ergebnisse und Diskussion: Die kompartmentelle Analyse von spross- und wurzel-respiriertem CO_2 von Pflanzen aus hohem Stickstoffversorgungsniveau ergab, dass die Respiration beider Organe im Wesentlichen von drei Substratpools mit Kohlenstoff versorgt wurde, die erhebliche Unterschiede bezüglich ihrer Halbwertszeiten aufwiesen. Während gut die Hälfte des respirierten Kohlenstoffs eine Kurzzeitspeicherung im größten Pool des Systems erfuhr, stellten zwei kleinere Substratpools, die sehr rasch von Assimilaten rezenter Photosynthese umgewälzt wurden, etwa 40% des respirierten Kohlenstoffs bereit. Langzeitspeicher waren in diesen Pflanzen als Kohlenstoffquelle von untergeordneter Bedeutung und konnten kinetisch nicht charakterisiert werden. Diese Sachverhalte hatten für Spross und Wurzel Gültigkeit, und nicht zuletzt dies deutete daraufhin, dass sowohl die Spross- als auch die Wurzelrespiration von denselben Substratpools versorgt wurde. Bei stickstofflimitierten Pflanzen konnte dasselbe Konzept des 3-Pool-Versorgungssystems der Respiration nachgewiesen werden. Dieses beinhaltete allerdings eine etwa 30% größere spezifische Menge an Kohlenstoff als jenes gut mit Stickstoff versorgter Pflanzen, und die Pool-Halbwertszeiten nahmen zum Teil erheblich zu. Des Weiteren fiel einem Langzeitspeicher eine wesentliche Rolle als Kohlenstofflieferant für die Respiration zu, was

insgesamt dazu führte, dass sich die Verweildauer von Kohlenstoff im respiratorischen Versorgungssystem von 1,6 Tagen bei hohem Stickstoffniveau auf knapp 6 Tage mit Stickstofflimitierung verlängerte.

Schlussfolgerungen: Mit vorliegender Arbeit wird erstmalig ein konzeptuelles Modell für das respiratorische Versorgungssystem von Deutsch Weidelgras vorgestellt, welches auf empirischem Beweis basiert. Es beinhaltet, dass die Komplexität des respiratorischen Substratstoffwechsels in Spross und Wurzel auf wenige wesentliche Komponenten (d.h. Kohlenstoffpools und Kohlenstoffflüsse) auf der Ebene der ganzen Pflanze reduziert werden konnte. Die Gültigkeit des Modells war nicht vom Stickstoffernährungszustand der Pflanzen beeinflusst, obwohl dieser zum Teil erhebliche Auswirkungen auf die Eigenschaften der respiratorischen Substratpools hatte. Die Verweildauer von Kohlenstoff im respiratorischen Versorgungssystem war stark von der Stickstoffversorgung abhängig und wurde hauptsächlich über Kohlenstoffflüsse zwischen Produkten rezenter Photosynthese und Kurzzeitspeichern (bei guter Stickstoffversorgung) bzw. Langzeitspeichern (bei Stickstoff-Limitierung) reguliert. Da der Großteil des respiratorischen Kohlenstoffs in oberirdischer Biomasse lokalisiert war, fiel möglicherweise dem Spross eine Kontrollfunktion der Kohlenstoffallokation im respiratorischen Versorgungssystem zu.

List of Figures

- Figure II.1: Time course of the fraction of unlabeled carbon in CO₂, respired by shoots (closed symbols) and roots (open symbols) of perennial ryegrass plants during respiration measurements, for plants that were previously labeled for 1 h (triangles) and 24 h (circles). Error bars denote ± 1 SE (n=4). The dashed line denotes the linear regression for shoots labeled for 1 h ($y = 0.83 + 0.48x$, $r^2 = 0.74$). The regression for the other labeling times was non-significant (not shown). 12
- Figure II.2: Specific respiration rates of shoots (closed symbols) and roots (open symbols) of perennial ryegrass, labeled for different time intervals, and of non-labeled controls (C, left panel). Each value is the mean of four to ten replicate plants (± 1 SD). Dashed lines indicate average values. Note the logarithmic scaling of the x-axis. 17
- Figure II.3: Evolution of the fraction of unlabeled carbon ($f_{\text{unlabeled}}$) in CO₂ respired by shoots (A) and roots (B) of perennial ryegrass during labeling. Each value is the mean of four to six replicate plants (± 1 SE). Lines denote model predictions (Fig. II.4). Insets expand the first 48 h. 18
- Figure II.4: Three-pool model of the substrate supply system of dark respiration of the shoot of perennial ryegrass. Carbon fixed in photosynthesis enters the respiratory system *via* pool Q₁, where it is either respired (respiratory flux F₁₀) or transferred to pool Q₂. In Q₂ carbon is either respired directly (F₂₀) or first cycles through Q₃ before being respired *via* Q₂. Respiratory tracer release from Q₂ is associated with a delay. Functional characteristics of the pools (size, half-life and contribution to shoot and root respiration; Table II.1) were estimated by translating the model into a set of differential equations, and fitting the model to the tracer kinetics of shoot respiration. The same model also fitted the tracer kinetics of dark respiration of the root, but included an additional delay of 0.8 h for tracer release in F₁₀ and F₂₀. Arrows and boxes are scaled to indicate the magnitude of fluxes and pool sizes. 19
- Figure II.5: Sensitivity of the goodness of model fits for the shoot (A-C) and the root (D-F) to departures from optimized values of pool size (A, D), half-life (B, E) and contribution to respiration (C, F). Sensitivity is expressed by the root mean squared error (RMSE) of the fit (minimum RMSE indicates the optimum value of a model parameter). The solid line represents Q₁, the dotted line Q₂, and the dashed line Q₃. Note the logarithmic scaling of the x-axis for pool size and half-life. 20
- Figure III.1: Total carbon mass of perennial ryegrass grown with a nitrogen supply of either 1.0 mM (open symbols) or 7.5 mM (closed symbols). Each value is the mean of 3-6 replicate plants. Lines denote linear regression ($p < 0.05$; see also Table III.1). Note the logarithmic scaling of the y-axis. 36
- Figure III.2: Specific respiration rates of perennial ryegrass grown with a nitrogen supply of either 1.0 mM (open symbols) or 7.5 mM (closed symbols), labeled for different time intervals, and of non-labeled controls (C; at left). Each value is the mean of 3-12 replicate plants (± 1 SE). Average rates were 46.3 ± 0.8 (n=56) and 35.7 ± 0.7 (n=60) for low- and high-nitrogen plants, respectively (dashed lines). Regression analysis yielded no significant trends ($p > 0.05$). Note the logarithmic scaling of the x-axis. 37

Figure III.3: Time course of tracer incorporation into CO₂ respired by perennial ryegrass plants grown with a nitrogen supply of either 1.0 mM (open symbols) or 7.5 mM (closed symbols) during labeling. Each value is the mean of 3-6 replicate plants (± 1 SE). Lines denote model predictions (Fig. III.4). Inset expands the first 48 h. The data points at 8 d labeling duration overlap. 38

Figure III.4: Compartmental model of the three pools supplying carbon to respiration of intact perennial ryegrass plants. Tracer enters the plant during photosynthesis and is respired *via* Q₁ (F₁₀) or Q₂ (F₂₀). ‘Delay’ means a lag between tracer acquisition by Q₂ and its release in respiration. Functional characteristics of the pools (Table III.2) were estimated by translating the model into a set of differential equations, and fitting the model to the tracer kinetics. 39

Figure III.5: Sensitivity of the quality of model fits for plants grown with a supply of either 1.0 mM nitrogen (A-C) or 7.5 mM (D-F) to variation of the optimized values of pool size (A, D), half-life (B, E) and contribution to respiration (C, F). Sensitivity is expressed by the root mean squared error (RMSE) of the fit (minimum RMSE indicates the optimum value of a model parameter). The solid line represents Q₁, the dotted line Q₂, and the dashed line Q₃. Note the logarithmic scaling of the x-axis for pool-size and half-life. 42

Figure IV.1: C isotope composition (δ) of CO₂ leaving the four growth chambers during one week of the experimental period. Values are hourly means of four measurements of individual chambers with stands of 6-week-old (upright and downright triangles) and 10-week-old (circles and diamonds) perennial ryegrass plants grown in either low or high supply of nitrogen, respectively. The standard deviation of the means never exceeds the symbols’ size. 47

Figure IV.2: Evolution of the fraction of unlabeled carbon in CO₂ respired by shoots (black symbols) and roots (open symbols) of perennial ryegrass during labeling. Each value is the mean of two to six replicate plants (± 1 SE). Inset expands the first 42 h. Plants were grown in the growth chamber system as described in chapters II and III, with a constant Temperature of 20 °C, relative humidity of 85%, 360 $\mu\text{L L}^{-1}$ [CO₂] and a nitrogen supply of 7.5 mM in the nutrient solution. Plants were grown in day/night-cycles with 16 h photoperiods (irradiance 425 $\mu\text{mol m}^{-2} \text{s}^{-1}$ PPFD at the top of the canopy) and 8 h dark periods, indicated by white and black horizontal bars. Shortly before the start of labeling at time 0 (*i.e.* the end of a dark period), when plants were 6-10 weeks old, the plants were subject to a severe defoliation, where all leaf blades were removed. Respiration measurements were carried out as described in chapters II and III. During the first light period following defoliation, virtually no tracer was detected in shoot- and root-respired CO₂. Thereafter, the fraction of unlabeled carbon in shoot-respired CO₂ decreased rapidly, and after 8 d of defoliation, it approximated 0. The fraction of unlabeled carbon in root-respired CO₂ only started to decrease in the second light period after defoliation, and it occurred at a slower rate than observed for the shoot. Two weeks after defoliation, 20% of root-respired CO₂ was still unlabeled. 51

List of Tables

- Table II.1: Optimization results for the parameters of the model shown in Figure II.4, as applied to the tracer time courses of shoot and root respiration (Fig. II.3). Model parameters include the size, half-life and percentage contribution to respiration of pools Q_1 , Q_2 and Q_3 . Together, the three pools accounted for 95% of shoot and root respiration. The remainder was supplied by sources which released no tracer within the 25 d-long labeling period (Fig. II.3). The quality of the fits is expressed as the root mean squared error (RMSE). 21
- Table III.1: Growth parameters of perennial ryegrass grown with either a low (1.0 mM) or a high (7.5 mM) supply of nitrogen. Values are means of 56 and 60 replicate plants for low and high nitrogen, respectively, ± 1 SE. Significant differences are based on a t-test, $***P \leq 0.001$ 36
- Table III.2: Optimized parameters (size, half-life and percentage contribution to respiration of pools Q_1 , Q_2 and Q_3) of the model shown in Figure III.4 fitted to tracer time-courses shown in Figure III.3. The quality of the fit is expressed as the root mean squared error (RMSE).40
- Table III.3: Content of water-soluble carbohydrate fractions of perennial ryegrass grown with either a low (1.0 mM) or a high (7.5 mM) supply of nitrogen. Values are means of six replicate plants ± 1 SE, along with the significance of the difference based on a t-test. $*P \leq 0.05$; NS, not significant, $P > 0.05$ 41

Chapter I: General Introduction

From both agronomical and ecological perspectives, knowledge about the trade-offs in resource allocation between the two essential requirements of plants is of particular interest: the need for growth (as the concept of plant competitiveness) and the need to survive and keep the organism in a functional state (including defense mechanisms against biotic and abiotic stress; Matyssek et al., 2002). However, the mechanisms that control and regulate the allocation of plants' external resources are not well understood. This is the core subject of the research association SFB 607 'Growth and Parasite Defense – Competition of Resources in Economic Plants from Forestry and Agronomy' (<http://www.sfb607.de>), which integrates work about resource allocation at physiological, biochemical and molecular scales.

The present work is part of this interdisciplinary research program with focus on carbon allocation at the whole plant level. In particular, it deals with the respiratory carbon supply system of perennial ryegrass (*Lolium perenne*), the most important C3 forage grass in temperate humid grasslands. Respiration is an integrated component of plants' carbon metabolism, which operates for both growth and maintenance functions. In terms of plants' carbon balance, respiration represents an expense of carbon, caused by the breakdown of organic compounds and the subsequent release of CO₂. Depending on species, developmental stage and growth conditions, 30–80% of the carbon provided by photosynthesis may be consumed by respiration (Dewar et al., 1998; Gifford, 2003; Van Iersel, 2003). In a physiological sense, however, this investment of carbon is essential, since it ultimately allows the growth and survival of plants by the conversion of assimilate into a usable form of energy (ATP) and reducing nucleotides (like NAD(P)H; ap Rees, 1980; Amthor, 1989; Fernie et al., 2004; Plaxton and Podestá, 2006). Respiration is furthermore a source of carbon skeletons, of building blocks for the biosynthesis of various organic compounds, and hence, respiration plays a decisive role in carbon allocation between the sinks that it serves.

Respiratory carbon metabolism is a highly complex network which involves several metabolic pathways including glycolysis, the TCA-cycle and the oxidative pentose phosphate pathway (Heldt, 2005). It operates in functionally distinct organs throughout the plant and a variety of biochemical compounds can serve as substrates for respiration (ap Rees, 1980; Heldt, 2005). Indeed, carbohydrates are usually considered as the biochemical compounds posing the major source of respired carbon (ap Rees, 1980; Tcherkez et al., 2003). But plants have the capacity to respire various substrates, like organic acids, proteins or fatty acids, though the latter may become important substrates particularly in conditions of carbohydrate

starvation (ap Rees, 1980; Brouquisse et al., 1991; Dieuaide-Noubhani et al., 1997; Tcherkez et al., 2003). Thus, the carbon in respired CO₂ may principally originate from a mixture of metabolic compounds, but it is actually not known how much each category contributes.

Besides a biochemical classification, substrate pools in general may as well be differentiated upon their functions within plants' carbon metabolism. They may act as short-term stores (to buffer temporary imbalances in resource supply, like in dark periods), long-term stores (*e.g.* to enhance regrowth after grazing or mowing), or they may involve substrate deriving directly from current photosynthesis, (*i.e.* substrate, that is transported to sinks immediately after photosynthetic fixation). It was repeatedly shown that carbon in respired CO₂ may originate from both current assimilation products and from stores. This was true for respiration of leaves (Nogués et al., 2004), for root systems of several herbaceous species (Kouchi et al., 1985; Lötscher and Gayler, 2005), and for respiration of ryegrass canopies (Schnyder et al., 2003). The functional identity of all substrate pools forming the respiratory supply system of a plant, however, is largely unknown. In grasses, both current assimilation products and stores also serve as substrates for growth (Lattanzi et al., 2005; Wild et al., unpublished results) and for root exudation (Dilkes et al., 2004). Thus, a mechanistic concept of the substrate supply systems serving different sinks may be based on the functional identification of their carbon pools. This could help to reveal the links between competing sinks at the level of substrate pools and improve the understanding of plant allocation patterns towards functionally distinct requirements. The aim of the present thesis was to identify the respiratory substrate pools and to develop a mechanistic model of the respiratory supply system of perennial ryegrass.

For the functional identification of pools one can take advantage of an inherent feature of metabolic carbon pools: they show turnover. Turnover implies that there is a flux of carbon atoms through pools, even when they remain at constant size, and pools of different functional-biochemical identity may turn over at different rates. These fluxes can be traced with isotope techniques without any relevant disturbance of biochemical and biophysical properties of the system. By changing the carbon isotopic composition of atmospheric CO₂, the photosynthetic fixation flux is altered (*i.e.* labeled) immediately, while the isotopic composition of the respiratory CO₂ efflux only starts to change once tracer arrives in the substrate pools supplying respiration. The time course of tracer incorporation into respired CO₂ carries information about the number and the characteristics of the pools involved.

Depending on the size of the system and the flux through it, however, substrate pools may exhibit turnover rates differing in several orders of magnitude. For a comprehensive

description of the whole system, labeling should ideally be conducted until the slowest turned over pool reaches a 'new' isotopic equilibrium, that is, when its carbon is fully exchanged with tracer. Principally, the long-lived radioactive isotope ^{14}C can be used in labeling studies. Since its first use by plant physiologists (Ruben and Kamen, 1941), ^{14}C labeling was often and successfully applied and served, for instance, to discover the path of carbon in photosynthesis (Calvin and Bassham, 1962; see Benson, 2002 for a historical overview of the early work with ^{14}C). The long-term labeling of big systems (like intact plants), however, would require large quantities of expensive ^{14}C and pose problems considering environmental health. For these reasons, labeling systems with stable carbon isotopes ($^{13}\text{C}/^{12}\text{C}$) have been developed (Deléens et al., 1983; Kouchi and Yoneyama, 1984; Geiger and Shieh, 1988; Schnyder, 1992; Schnyder et al., 2003). They are safe to use and take advantage of the differences in the abundance of ^{13}C in atmospheric CO_2 and that of commercially available, less expensive CO_2 .

For the assessment of system dynamics with stable isotopes of carbon, discrimination processes caused by kinetic and equilibrium isotope effects have to be taken into account. They occur in carbon exchange mechanisms of metabolic pathways and in gas exchange processes between the atmosphere and the plant (Park and Epstein, 1961; Farquhar and Richards, 1984; Gleixner et al., 1993; Ghashghaie et al., 2003), the latter being sensitive to growth conditions like water availability (Farquhar and Richards, 1984; Schnyder et al., 2006), irradiance (Hanba et al., 1997) or nitrogen supply (Sparks and Ehleringer, 1997; Hikoska et al., 1998). Since labeling with stable isotopes requires the detection of relatively small differences in $^{13}\text{C}/^{12}\text{C}$ ratios, discrimination effects could potentially alter the isotopic signature of the carbon fixed in photosynthesis and hence, bias the estimation of the amount of tracer and so the system dynamics.

For the experiments described in the present thesis, a dynamic labeling approach was used and the time course of tracer incorporation in respired CO_2 served to develop the mechanistic concept of the respiratory supply system of perennial ryegrass. The experiments were conducted in controlled growth facilities as described by Schnyder et al. (2003). All critical aspects of labeling with $^{13}\text{CO}_2/^{12}\text{CO}_2$ could be fully accounted for, *inter alia* by keeping the environmental conditions for the plants constant throughout the experiments. With the use of modern gas-exchange measurement techniques, the expression of the carbon isotope discrimination was assessed online and (near) continuously to ensure that plants were growing in isotopic equilibrium before the onset of labeling. The change in the isotopic signature in respired CO_2 with labeling could therefore be assigned purely to tracer content

and was not caused by other effects. Thus, the conceptual model of the respiratory supply system of perennial ryegrass could be developed and validated with so far not attained reliability.

Chapter II describes an experiment, where in plants grown with a full supply of nitrogen, three major substrate pools that supply carbon to respiration of the shoot and the root were identified. A concept for the network architecture of the pool system at the plant level is provided. In a next step, the variability of substrate pool characteristics was tested experimentally by comparing the respiratory supply systems of plants that grew continuously in contrasting levels of nitrogen fertilization with otherwise identical growth conditions. This is the subject of chapter III. At the end of the thesis, a summarizing discussion is given, including the reliability of the present findings for systems in which a steady-state growth is not given.

Chapter II: Root and Shoot Respiration of Perennial Ryegrass Are Supplied by the Same Substrate Pools: Assessment by Dynamic ^{13}C Labeling and Compartmental Analysis of Tracer Kinetics ¹

ABSTRACT

The substrate supply system for respiration of the shoot and root of a perennial grass was characterized in terms of component pools, and pool's functional properties: size, half-life ($t_{1/2}$) and contribution to respiration of the root and shoot. The investigations were performed with *Lolium perenne* L. growing in constant conditions with continuous light. Plants were labeled with $^{13}\text{CO}_2/^{12}\text{CO}_2$ for periods ranging from 1 h to 600 h, followed by measurements of the rates and $^{13}\text{C}/^{12}\text{C}$ ratios of CO_2 respired by shoots and roots in the dark. Label appearance in roots was delayed by approximately 1 h relative to shoots; otherwise the tracer time course was very similar in both organs. Compartmental analysis of respiratory tracer kinetics indicated that, in both organs, three pools supplied 95% of all respired carbon (a very slow pool whose kinetics could not be characterized provided the remaining 5%). Pool's half-lives and relative sizes were also near-identical in shoot and root ($t_{1/2} < 15$ min, ~ 3 h and 33 h). An important role of short-term storage in supplying respiration was apparent in both organs: only 43% of respiration was supplied by current photosynthate (fixed carbon transferred directly to centers of respiration *via* the two fastest pools). The residence time of carbon in the respiratory supply system was practically the same in shoot and root. From this and other evidence, we argue that both organs were supplied by the same pools, and that the residence time was controlled by the shoot *via* current photosynthate and storage deposition/mobilization fluxes.

¹ Lehmeier CA, Lattanzi FA, Schäufole R, Wild M, Schnyder H (2008) Plant Physiology, Vol. 148, pp. 1148-1158. DOI: 10.1104/pp.108.127324

INTRODUCTION

This paper deals with the substrate supply system of respiration in roots and shoots of intact plants of a perennial grass, *Lolium perenne* L. This system is an integral part of the total pool of available substrates for growth and maintenance processes in the root and shoot, and a major sink for carbon fixed in photosynthesis (Amthor, 1989). In the narrow sense, respired carbon mainly derives from a few compounds: malate, pyruvate, isocitrate, α -ketoglutarate or gluconate 6-phosphate (Heldt, 2005), which together account for only a small fraction of total plant biomass. Conversely, in the broad sense, all respired carbon derives from photosynthesis and, ultimately, most of the carbon fixed in photosynthesis is returned back to the atmosphere by way of respiration (Schimel, 1995; Trumbore, 2006). Before being respired carbon may visit various biochemical compounds in different organs. In principle, the physical and biochemical paths taken by carbon before being used as a substrate in respiration can be intricate, reflecting the physical and biochemical complexity of plant metabolic networks (ap Rees, 1980; Plaxton and Podestá, 2006).

The intermediary fate (or allocation history) of carbon controls its residence time inside the plant (that is, the lapse of time between fixation and respiration). Thus, for instance, if carbon fixed in photosynthesis is transferred directly to centers of respiration, then the residence time in the plant is short (seconds to minutes). In contrast, if carbon is first deposited in long-lived molecules (such as proteins or storage carbohydrates) then the residence time is long (days to months). Respired carbon therefore originates from a heterogeneous mixture of molecules which cycle more or less extensively through a network of biochemical compounds and physical compartments. So, the residence time of respired carbon reveals functional properties of the supply system feeding respiration, and can be used to shed light on structural-functional differences between supply systems feeding different plant parts, such as roots and shoots. We are not aware of any comparative studies of the residence time of carbon feeding shoot and root respiration.

The residence time of carbon can be characterized by quantitative tracer techniques (Ryle et al., 1976; Kouchi et al., 1985; Schnyder et al., 2003; Lötscher and Gayler, 2005). Studies at the level of whole plants (Schnyder et al., 2003) or with root systems (Kouchi et al., 1985; Kouchi et al., 1986; Lötscher and Gayler, 2005) have revealed two distinct phases in the kinetics of tracer appearance in respired CO₂: a phase with fast label appearance, which indicated a supply component that was closely connected with current photosynthetic activity, and a phase with slow label appearance, which indicated the participation of one (or more) store(s) in supplying respiration. Several types of compounds, including starch, vacuolar

sucrose and fructan, as well as proteins have been suggested as stores supplying substrates for respiration (ap Rees, 1980; Farrar, 1980). It is unknown if the contribution of stores and products of current assimilation to respiration is the same or different in shoots and roots.

Whereas most of the interpretations of label appearance (in dynamic labeling) – or label disappearance (in pulse-chase labeling) – in respired CO₂ have been qualitative, the tracer kinetics can also be quantitatively and mechanistically interpreted in terms of the number, size, kinetic properties (half-life, turnover rate) and contribution of the pools which compose the supply system of respiration. This is best done using the mathematical methodology of compartmental analysis (Atkins, 1969; Jacquez, 1996), which has been applied to various problems of the assimilation, transport and metabolism of carbon in plants (for instance, Moorby and Jarman, 1975; Prosser and Farrar, 1981; Rocher and Prioul, 1987; Bürkle et al., 1998; Lattanzi et al., 2005). A pool is defined here as a set of compounds which exhibit the same proportion of labeled carbon atoms; that is a pool represents a ‘space’ in which the isotopic composition is uniform (see *e.g.* Rescigno, 2001). So, in principle, one pool can include several populations of anatomical (physical) features and biochemical species on the condition that they exhibit the same proportion of label. Most importantly, however, by characterizing the pool on the basis of respiratory tracer release, the pool is identified by its function, namely supplying respiration with substrate.

Here, we use compartmental analysis to provide a quantitative description and comparison of the compartmental structure and kinetic properties of the supply system feeding root and shoot respiration. Specifically, we address the following questions: What are the kinetics and sizes of the major respiratory pools supplying carbon to respiration of ryegrass (*Lolium perenne* L.)? How are these pools connected? How do shoot and root differ in terms of carbon supply by those pools? And, what are the contributions of current assimilation and stores to respiration?

One basic difficulty in the characterization of carbon pools supplying respiration is a sufficient range of tracer application (or chase) times. Putative substrates for respiration have turnover times in the range of <1 h to many days (Simpson et al., 1981; Dungey and Davies, 1982; Farrar and Farrar, 1986; Rocher and Prioul, 1987; Schnyder et al., 2003) or possibly weeks, meaning that labeling (or chase) times must vary by about four orders of magnitude, if all components of the respiratory supply system are to be characterized. Typically, however, the range of tracer exposure (or chase) times has been much narrower, thus capturing only fast or slow pools. In this study, we aimed to characterize all major components of the respiratory supply system by using labeling times ranging from 1 to 600 h. To this end, we labeled all

carbon assimilated by individual plants with a known constant $^{13}\text{C}/^{12}\text{C}$ ratio in CO_2 over a period of up to 25 days, when respired CO_2 had reached 95% label saturation [this labeling method is termed ‘steady-state labeling’ in ‘classical’ plant physiology literature (*e.g.* Geiger and Swanson, 1965; Geiger et al., 1969), but is now referred to as ‘dynamic labeling’ (Ratcliffe and Shachar-Hill, 2006)]. The $^{13}\text{C}/^{12}\text{C}$ ratio of respiratory CO_2 produced in the root and shoot was measured at various times, and the time course of tracer in respired CO_2 was evaluated with compartmental analysis.

MATERIALS AND METHODS

Plant material and growth conditions

Seeds of perennial ryegrass (*Lolium perenne*, cv. Acento) were sown individually in plastic pots (350 mm height, 50 mm diameter) filled with 800 g of washed quartz sand (0.3 - 0.8 mm grain size). The bottom of every pot had a drainage hole (7 mm diameter) covered with a fine nylon net. Pots were arranged in plastic containers (760 x 560 x 320 mm) at a density of 378 plants m^{-2} . Two containers were placed in each of two growth chambers (Conviron E15, Conviron, Winnipeg, Canada). Plants were grown in continuous light, supplied by cool white fluorescent tubes. Irradiance was maintained at $275 \mu\text{mol m}^{-2} \text{s}^{-1}$ PPFD at the top of the canopy. Temperature was controlled at $20 \text{ }^\circ\text{C}$ and relative humidity near 85%. The stands were irrigated by flooding the boxes every 3 h briefly with modified Hoagland solution (2.5 mM $\text{Ca}(\text{NO}_3)_2$, 2.5 mM KNO_3 , 1.0 mM MgSO_4 , 0.18 mM KH_2PO_4 , 0.21 mM K_2HPO_4 , 0.5 mM NaCl , 0.4 mM KCl , 0.4 mM CaCl_2 , 0.125 mM Fe as EDTA, and micronutrients). Stands were periodically flushed with demineralized water to prevent salt accumulation.

CO_2 control in the growth chambers

The two growth chambers formed part of the $^{13}\text{CO}_2/^{12}\text{CO}_2$ gas exchange and labeling system described by Schnyder et al. (2003). Air supply to the chambers was performed by mixing CO_2 -free air and CO_2 with known carbon isotope composition ($\delta^{13}\text{C}$, with $\delta^{13}\text{C} = [({}^{13}\text{C}/{}^{12}\text{C}_{\text{sample}}) / ({}^{13}\text{C}/{}^{12}\text{C}_{\text{international VPDB standard}})] - 1$), using mass flow controllers. Control was facilitated by measuring concentration and $\delta^{13}\text{C}$ of CO_2 online every 20 – 30 min by an infrared gas analyzer (IRGA, Li-6262, Li-Cor Inc., Lincoln, NE, USA) and a continuous-flow isotope-ratio mass spectrometer (CF-IRMS, Delta Plus, Finnigan MAT, Bremen, Germany).

One chamber received ^{13}C -depleted CO_2 ($\delta^{13}\text{C} -28.8\text{‰}$), and the other ^{13}C -enriched CO_2 ($\delta^{13}\text{C} -1.7\text{‰}$) (both from Linde AG, Höllriegelskreuth, Germany). The $\delta^{13}\text{C}$ and concentration of CO_2 ($360 \mu\text{L L}^{-1}$) inside the chambers were kept near constant by

periodically adjusting airflow and CO₂ concentration in the inlet air of each chamber. The rate of CO₂ supply to the chambers exceeded the CO₂ exchange rate of the plant stands by a factor of 9. This minimized effects of photosynthesis and respiration on $\delta^{13}\text{C}$ and concentration of CO₂ in the chambers and suppressed the recycling of respiratory CO₂.

Chamber doors were equipped with custom-made transparent air-locks which had small ports through which plants could be handled and sampled. These air-locks assured minimal disturbance of the $\delta^{13}\text{C}$ and concentration of CO₂ in the chamber atmosphere when chambers had to be opened during the experiment. Empty chamber tests of air-locks demonstrated that with doors opened for 20 min, the CO₂ concentration in the chambers changed by only 4 $\mu\text{L L}^{-1}$, and $\delta^{13}\text{C}$ by about 1%. Twenty minutes after closing the chambers, CO₂ concentration and $\delta^{13}\text{C}$ in the chambers had returned to set-point values.

¹³C labeling

From three weeks after imbibition of seeds, when plants had three tillers, individual plants were labeled by swapping randomly selected plants between chambers. Thus, plants growing in the chamber with ¹³C-enriched CO₂ were transferred to the chamber with ¹³C-depleted CO₂, and *vice versa*. Plants were kept in the presence of the ‘new’ CO₂ for 1, 2, 4, 8 or 16 h; or for 1, 2, 4, 8, 12, 17 or 25 d. At the end of given labeling intervals, plants were removed from the stands and transferred to a root/shoot respiration measurement system. This was done for at least 4 replicate plants for each labeling interval. To minimize possible size- and development-related effects on respiration, labeling periods were scheduled in such a way that labeling duration and plant age at sampling were not correlated.

Respiration measurements

Shoot and root respiration rates as well as the $\delta^{13}\text{C}$ of shoot- and root-respired CO₂ of individual plants were measured in the gas exchange system described and used by Lötscher et al. (2004) and Klumpp et al. (2005). This system included four single-plant cuvettes interfaced to an IRGA and CF-IRMS *via* Teflon tubes. The cuvettes were kept in a temperature-controlled cabinet held at the same temperature as the two growth chambers. Each cuvette consisted of an open cylinder (200 mm height, 153 mm diameter) and a top and bottom plate (all made of polyvinylchloride), which could be opened and closed quickly to insert a pot. The bottom plate contained a duct that matched exactly the cross-sectional area of the pot. A similar system was used to seal the bottom of the pot. Rubber seals and vacuum grease ascertained that cuvettes were air-tight. Air with known constant $\delta^{13}\text{C}$ (-5‰) and

concentration of CO₂ (223 μL L⁻¹) was supplied to the cuvettes at a rate of 0.75 L min⁻¹ after passage of a humidifier. Air flow was controlled by mass flow controllers. Each cuvette had two outlets: one in the shoot section on the opposite side of the inlet, and the other at the bottom of the pot which enclosed the root compartment. Air in the shoot compartment was ventilated by a fan. Part of the air stream feeding the shoot compartment (0.25 L min⁻¹) was drawn through the root compartment with a gas-tight Teflon-lined peristaltic membrane pump. The air was then dried and the flow to a multi-way valve block (sample air selector, SAS) controlled by a mass flow controller. The remaining air from the shoot compartment was directly conveyed to the SAS. A reference air line (0.9 L min⁻¹) was also connected to the SAS. The SAS sequentially sampled the reference air line and the eight sample air lines and fed the air to the IRGA and CF-IRMS as described in Schnyder et al. (2003).

Prior to measurements, just after removal from the growth chambers, the pots were rinsed with demineralized water, which was previously aerated with CO₂-free air for one day. Plants were then enclosed in the respiration cuvettes and the cuvettes flushed with CO₂-free air. After excess water had drained off the bottom section of the cuvette, all measuring air lines were installed and air flow rates were adjusted, as described above. These procedures aimed at removing all extraneous air from shoot and root compartments as quickly as possible.

A full measurement cycle of all four cuvettes was completed in ~45 min and included three replicate measurements of δ¹³C and concentration of CO₂ in the air exiting the shoot and root compartment of each cuvette *plus* one reference air measurement. Dark respiration of shoot and root was recorded for about 5 h, thus yielding six full measurements for each plant (*cf.* Fig. II.1). First reliable measurements of the rates and δ¹³C of shoot respiration were obtained ~30 min after removing plants from the stands, but it took up to 1.5 h to purge the root system free of all extraneous CO₂ (*cf.* Lötscher et al., 2004). Therefore, it can be ruled out that photorespiratory CO₂ release has contributed to the measured isotopic signal, since the time to purge the cuvettes previous to measurements was much longer than the duration of the (photorespiratory) post-illumination burst. Each δ¹³C sample was measured against a working gas standard which was previously calibrated against a VPDB-gauged laboratory CO₂ standard. The standard deviation of repeated single measurements was 0.10‰ for δ¹³C and 0.34 μL L⁻¹ for the concentration of CO₂ on average of all measurements. The respiration rate of roots decreased slightly (~6%) during the 5 h measurement period, while that of shoots was constant. Average rates were used to calculate specific respiration rates on a carbon basis.

Plant harvest and elemental analysis

Immediately after the termination of respiration measurements, plants were removed from the pots, washed free of sand, dissected into shoot and root, weighed, frozen in liquid nitrogen, and stored at -30 °C. All samples were freeze-dried for 72 h, weighed again, and ground to flour mesh quality in a ball mill. Aliquots of $0.75 \text{ mg} \pm 0.05 \text{ mg}$ of each sample were weighed into tin cups (IVA Analysentechnik e.K., Meerbusch, Germany) and combusted in an elemental analyzer (Carlo Erba NA 1110, Carlo Erba Instruments, Milan, Italy), interfaced to the CF-IRMS, to determine carbon and nitrogen contents.

Analysis of water-soluble carbohydrates

Water-soluble carbohydrates were extracted and quantified as described by Schnyder and de Visser (1999).

Data analysis

The proportion of carbon in shoot- and root-respired CO_2 that was assimilated before (unlabeled) and during labeling, $f_{\text{unlabeled-C}}$ and $f_{\text{labeled-C}}$ (where $f_{\text{labeled-C}} = 1 - f_{\text{unlabeled-C}}$), was calculated as by Schnyder and de Visser (1999):

$$(1) \quad f_{\text{unlabeled-C}} = (\delta^{13}\text{C}_S - \delta^{13}\text{C}_{\text{new}}) / (\delta^{13}\text{C}_{\text{old}} - \delta^{13}\text{C}_{\text{new}}),$$

where $\delta^{13}\text{C}_S$, $\delta^{13}\text{C}_{\text{old}}$ and $\delta^{13}\text{C}_{\text{new}}$ are the $\delta^{13}\text{C}$ of respiratory CO_2 produced by the labeled sample plant, and non-labeled plants growing continuously in the chamber of origin ('old') or in the labeling chamber ('new'). $\delta^{13}\text{C}_S$, $\delta^{13}\text{C}_{\text{old}}$ and $\delta^{13}\text{C}_{\text{new}}$ of shoots were obtained as

$$(2) \quad \delta^{13}\text{C}_X = (\delta^{13}\text{C}_{\text{in}} F_{\text{in}} - \delta^{13}\text{C}_{\text{out}} F_{\text{out}}) / (F_{\text{in}} - F_{\text{out}}),$$

where X stands for 'sample', 'new' or 'old' (as appropriate), and $\delta^{13}\text{C}_{\text{in}}$, $\delta^{13}\text{C}_{\text{out}}$, F_{in} and F_{out} are the isotopic signatures and the flow rates of the CO_2 entering and leaving the shoot cuvette, respectively. Calculations for the root compartment were done in the same way in considering that the concentration and $\delta^{13}\text{C}$ of the CO_2 entering the root compartment was equal to that in the shoot compartment (*cf.* Klumpp et al., 2005).

The $\delta^{13}\text{C}$ of shoot-respired CO_2 of individual control plants as well as that of labeled plants did not change during the 5 h of respiration measurements ($p > 0.05$). From 1.5 h after transfer the $\delta^{13}\text{C}$ of root respiration was also stable (*cf.* Fig. II.1). Barbour et al. (2007) have

observed rapid and pronounced changes in $\delta^{13}\text{C}$ of respired CO_2 during the first few minutes following light-to-dark transition in *Ricinus communis* L. We did not observe such effects, probably because first measurements started 30 minutes after removal from the chamber. Thus, $\delta^{13}\text{C}$ of respiratory CO_2 of the shoot or root of one plant was taken as the mean of all the measurements of a plant. This was true for all measurements, except for shoots labeled for only 1 h: in these $f_{\text{unlabeled-C}}$ increased markedly during the measurement (Fig. II.1), suggesting depletion of a rapidly labeled carbon pool. In that case, regression analysis was applied and $f_{\text{unlabeled-C}}$ was taken as the y-intercept of the linear regression of $f_{\text{unlabeled-C}}$ (y) versus time after removal from the growth chamber (x) (Fig. II.1). This procedure ensured that $f_{\text{unlabeled-C}}$ in shoot- and root-respired CO_2 of each plant referred to the same time in darkness and provided thus the basic reference points for the estimation of pool properties.

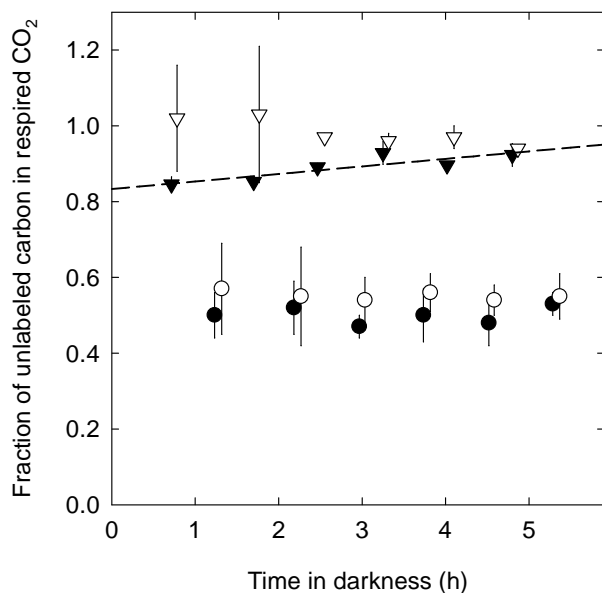


Figure II.1: Time course of the fraction of unlabeled carbon in CO_2 , respired by shoots (closed symbols) and roots (open symbols) of perennial ryegrass plants during respiration measurements, for plants that were previously labeled for 1 h (triangles) and 24 h (circles). Error bars denote ± 1 SE ($n=4$). The dashed line denotes the linear regression for shoots labeled for 1 h ($y = 0.83 + 0.48x$, $r^2 = 0.74$). The regression for the other labeling times was non-significant (not shown).

Carbon isotope discrimination, $\Delta^{13}\text{C}$ (defined as $\Delta^{13}\text{C} = (\delta^{13}\text{C}_{\text{CO}_2} - \delta^{13}\text{C}_{\text{respiratory CO}_2}) / (1 + \delta^{13}\text{C}_{\text{respiratory CO}_2})$), was determined for non-labeled plants from both chambers. Chambers did not differ ($p>0.05$), as would be expected from the fact that growth conditions were the same. However, there was a difference in $\Delta^{13}\text{C}$ of shoots and roots ($23.2\% \pm 1.0$ SD versus $25.8\% \pm 0.7$ SD), consistent with the observations of Klumpp et al. (2005). This effect was accounted for in the labeling data evaluation by using shoot- and root-specific $\delta^{13}\text{C}_{\text{new}}$ and $\delta^{13}\text{C}_{\text{old}}$ values in eqn 1 (above, see also Schnyder and de Visser, 1999).

Refixation of respiratory CO_2 was considered unimportant in this work. Principally, there are two aspects of refixation which are potentially relevant: one relates to refixation of respiratory CO_2 that has been released into the chamber atmosphere, the other concerns

(internal) re-fixation within the photosynthetic tissue. Re-fixation of respired CO_2 from the chamber atmosphere was insignificant in this open, rapidly turned over system, in which the rate of CO_2 supply to the chambers exceeded the stand CO_2 exchange rate by a factor of 9. The carbon isotope composition of CO_2 in the chamber air was measured near-continuously, and these measurements were taken as the actual source CO_2 isotope composition. Moreover, the small number of labelling plants present in a chamber at any moment had no measurable effect on the isotopic composition of CO_2 in chamber air. Internal re-fixation was estimated using knowledge of ^{13}C discrimination in shoot biomass, and assumptions about the fractional contribution of leaf respiration to stand respiration, and the ratio of respiration to photosynthesis. With a ^{13}C discrimination of 23.0‰, the c_i/c_a ratio (the ratio of leaf internal to atmospheric CO_2 concentration) of leaves was near 0.82 (Farquhar et al., 1989), thus the probability for re-fixation of leaf-respired CO_2 was approx. 18%. Assuming that leaf-respired carbon accounted for about one third of plant respiration, and that total plant respiration in light was one third of the photosynthetic flux, the contribution of re-fixation to total photosynthetic CO_2 fixation was approx. 1.6% ($0.18 \times 0.3 \times 0.3 = 0.016 = 1.6\%$). This effect was considered insignificant.

Compartmental modeling of tracer time course in respired CO_2

The model shown in Fig. II.4 was described mathematically assuming that the system was in steady-state, an assumption supported by constant specific growth and respiration rates of shoots and roots. Estimated turnover rates and half-lives assume first-order kinetics.

The fraction of tracer in each compartment with respect to time was given by:

$$(3a) \quad f_{\text{unlabeled-C-Q1}} = (Q_1 * f_{\text{unlabeled-C-Q1}} + F_{\text{In}} * f_{\text{labeled-C}} - F_{10} * f_{\text{unlabeled-C-Q1}} - F_{12} * f_{\text{unlabeled-C-Q1}}) / Q_1$$

$$(3b) \quad f_{\text{unlabeled-C-Q2}} = (Q_2 * f_{\text{unlabeled-C-Q2}} + F_{12} * f_{\text{unlabeled-C-Q1}} + F_{32} * f_{\text{unlabeled-C-Q3}} - F_{23} * f_{\text{unlabeled-C-Q2}} - F_{20} * f_{\text{unlabeled-C-Q2}}) / Q_2$$

$$(3c) \quad f_{\text{unlabeled-C-Q3}} = (Q_3 * f_{\text{unlabeled-C-Q3}} + F_{23} * f_{\text{unlabeled-C-Q2}} - F_{32} * f_{\text{unlabeled-C-Q3}}) / Q_3$$

$$(3d) \quad f_{\text{unlabeled-C}} = (F_{10} * f_{\text{unlabeled-C-Q1}} + F_{20} * f_{\text{unlabeled-C-Q2}}) / (F_{10} + F_{20}),$$

where Q_1 , Q_2 and Q_3 are the pool sizes and F_{In} is the flux of photosynthetically assimilated carbon (tracer) that enters the respiratory system. Since the system is in steady-state, and F_{In} equals the specific respiration rate, $F_{\text{In}} = F_{\text{Out}}$, $F_{\text{Out}} = F_{10} + F_{20}$ (Fig. II.4), $F_{12} = F_{20}$ and $F_{23} = F_{32}$. Indices refer to donor and receptor pools, respectively. Index 0 represents the

environment. The fraction of unlabeled carbon in shoot- or root-respired CO₂ is $f_{\text{unlabeled-C}}$. This is the measured parameter against which the model prediction is compared. $f_{\text{unlabeled-C-Q}_i}$ is the fraction of unlabeled carbon in the pool Q_i, $f_{\text{labeled-C}}$ is the constant fraction of fully labeled carbon entering the system after start of labeling.

In order to fit the initial part of the tracer time-course observed in root respiration, a Delay 2 was inserted between the beginning of labeling and the start of tracer incorporation into Q₁. In other words, tracer entered Q₁ in the root model a little later than in the shoot model, which would account for phloem transport time from shoot to root. Delay 2 was not necessary to simulate the tracer time-course observed in shoot respiration.

To model the stable degree of labeling in the first hours (Fig. II.3, insets), a Delay 1 between tracer acquisition in pool Q₂ and its efflux in F₂₀ (Fig. II.4) was required in both shoot and root simulations. Mathematically, $f_{\text{unlabeled-C-Q}_2}$ in eqn. 3d was forced to lag temporally behind $f_{\text{unlabeled-C-Q}_2}$ in eqns. 3b and c for the numerical value of Delay 1. Since Delay 1 operated only on the release side of Q₂ (*i.e.* F₂₀), it had no effect on the estimation of the half-lives of Q₂ and Q₃. Considering the steady-state of the system, it is important to note that Delay 1 and Delay 2 only apply to tracer content in respired CO₂, and not to the rate of respiration itself.

These equations were implemented in a custom-made program using the free software ‘R’ (R Development Core Team, 2007). Initial values for pool sizes, fluxes between pools and delays were inserted, and the set of numerical equations (3) was solved. In that way, a tracer time course across the entire labeling period (600 h) was generated. The goodness of the fit was expressed as the root mean squared error (RMSE):

$$(4) \quad RMSE = \sqrt{\frac{\sum_{i=1}^n (x(t_i) - X(t_i))^2}{n}},$$

with x and X the observed and model-predicted $f_{\text{unlabeled-C}}$ at labeling time i , and n the number of labeling times.

This procedure was followed many times by stepwise and systematic variation of pool sizes, fluxes and delays to identify the combination of values yielding the minimum RMSE (Table II.1, Fig. II.5).

Optimized pool sizes and fluxes served to calculate the half-life of a pool of size Q_i:

$$(5) \quad t_{1/2}(Q_i) = \ln(2) / (F_i / Q_i),$$

with F_i the sum of all fluxes leaving the pool Q_i .

Based upon optimized fluxes, the contribution of a pool Q_i (C_{Q_i}) to respiratory carbon release was derived, which is defined here as the probability of tracer moving in a certain flux of the respiratory system (cf. Fig. II.4):

$$(6a) \quad C_{Q_1} = F_{10} / (F_{10} + F_{12})$$

$$(6b) \quad C_{Q_2} = (1 - F_{10} / (F_{10} + F_{12})) * F_{20} / (F_{20} + F_{23})$$

$$(6c) \quad C_{Q_3} = (1 - F_{10} / (F_{10} + F_{12})) * F_{23} / (F_{20} + F_{23})$$

$$\text{and } C_{Q_1} + C_{Q_2} + C_{Q_3} = 0.95$$

C_{Q_1} is thus the probability that tracer enters the system and leaves it in F_{10} without visiting any other pool. C_{Q_2} implies, that tracer enters Q_2 *via* Q_1 and is respired in F_{20} without moving through Q_3 . C_{Q_3} is the probability of tracer cycling through the storage pool at least once.

Validity of model assumptions

As is the general case for compartmental analyses (*e.g.* Farrar, 1990; Lattanzi et al., 2005) the present one was based on the assumptions, that (1) the system is in a steady-state, (2) fluxes obey first-order kinetics and (3) pools are homogeneous and well mixed (Farrar, 1990; Lattanzi et al., 2005). Assumption (1) was well satisfied in the experiment: specific growth and respiration rates of shoots and roots were constant (see Results and Discussion). Also, the carbon to nitrogen ratio of biomass (24:1) did not change ($p > 0.05$, data not shown). Growing plants in continuous light ensured that short-term changes of pool sizes and fluxes (which are common to plants growing in day/night cycles) did not occur. Assumption (2) is probably false in a strict sense, but its practical validity seems supported (see Farrar, 1990 for a discussion).

Assumption (3) is perhaps the most drastic simplification in the model. Probably, the different pools are not truly homogeneous, but may comprise several biochemical compounds located in different spatial compartments, such as protein and fructan pools in different leaves. However, further compartmentalization did not improve goodness of fit, indicating that the kinetic properties of the components of a pool were similar. The observed lags for tracer arrival in the root and respiratory carbon release from Q_2 represent exemptions from the well-mixing assumption, which were explicitly accounted for by inserting (and optimizing) appropriate delays.

Tracer studies normally assume that isotopic discrimination in pool exchange processes can be neglected. In the present study, any effects of carbon isotope fractionation during photosynthesis, transport and metabolism on carbon isotope composition of respired CO₂ were accounted for in the evaluation of labeling data by assessing (and correcting for) isotopic discrimination in unlabeled plants (see de Visser et al., 1997).

RESULTS

Meeting the steady-state conditions of compartmental analysis: constant specific growth and respiration rates

Inferring the number and kinetics of mixing pools by compartmental analysis relies on several assumptions (see above). A major one is that the system under consideration shows no change in time except for tracer content (referred to as ‘metabolic steady-state’ by Ratcliffe and Shachar-Hill, 2006). By performing the present study in controlled environments, constant growth conditions were provided: plants grew with continuous illumination, and temperature, relative humidity and CO₂ concentration were maintained at constant values throughout the experiment. Water and nutrients were supplied frequently.

During the experiment, shoots and roots exhibited constant specific growth rates (shoot: $0.085 \text{ g C g}^{-1} \text{ shoot-C d}^{-1} \pm 0.011 \text{ CI}_{0.95}$, root: $0.072 \text{ g C g}^{-1} \text{ root-C d}^{-1} \pm 0.014 \text{ CI}_{0.95}$). Moreover, specific respiration rates were steady throughout the labeling period ($p > 0.05$; Fig. II.2), with shoot respiration ($0.97 \text{ mg C g}^{-1} \text{ plant-C h}^{-1} \pm 0.13 \text{ SD}$, $n=60$) being nearly twice as high as root respiration rates ($0.53 \text{ mg C g}^{-1} \text{ plant-C h}^{-1} \pm 0.09 \text{ SD}$, $n=60$). Further, due to the similarity of shoot and root specific growth rates, the shoot to root ratio ($3.8 \text{ g C g}^{-1} \text{ C}$) was near constant. No differences in the rates of growth and respiration were observed between growth chambers ($p > 0.05$). These results indicate that plants were growing near exponentially, with constant specific demands on respiration, and thus the system was virtually in a steady-state.

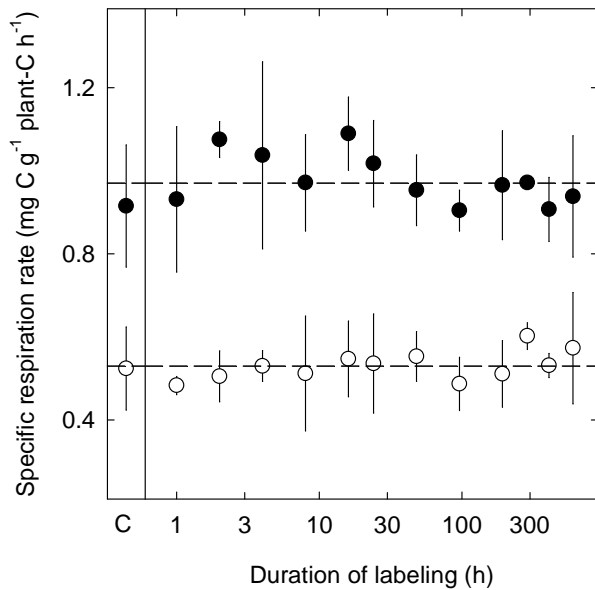


Figure II.2: Specific respiration rates of shoots (closed symbols) and roots (open symbols) of perennial ryegrass, labeled for different time intervals, and of non-labeled controls (C, left panel). Each value is the mean of four to ten replicate plants (± 1 SD). Dashed lines indicate average values. Note the logarithmic scaling of the x-axis.

Water-soluble carbohydrate concentration in root and shoot biomass

Water-soluble carbohydrates (WSC) accounted for 0.337 g C g^{-1} of total shoot-C (± 0.035 SD, $n=6$). This was more than four times higher than the concentration in the roots ($0.079 \text{ g WSC-C g}^{-1}$ root-C ± 0.006 SD, $n=6$).

Labeling kinetics of respired CO_2 in the shoot and root

The time courses of tracer incorporation into shoot- and root-respired CO_2 were strikingly similar (Fig. II.3), except that first label incorporation into respiratory CO_2 of roots occurred with a delay of approximately 1 h, and that the degree of labeling of root-respired CO_2 was about 5% less than that of shoots during the first week of labeling.

The labeling kinetics revealed five distinct phases: (i) a fast initial labeling, (ii) a lag period of a few hours in which the degree of labeling did not change (Fig. II.3, insets), (iii) a period which lasted until about 1 d of labeling in which the fraction of unlabeled carbon decreased rapidly, (iv) a period until about 8 d in which the fraction of unlabeled carbon decreased at a slower rate, and (v) a final period which lasted until the end of the experiment (25 d of labeling) in which the fraction of unlabeled carbon in respiration remained near 5% (Fig. II.3).

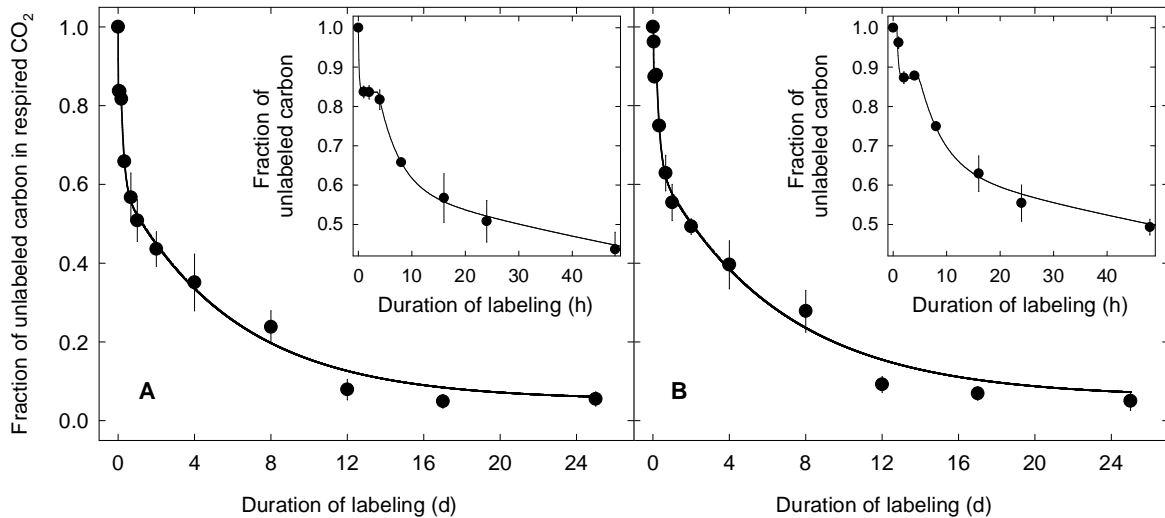


Figure II.3: Evolution of the fraction of unlabeled carbon ($f_{\text{unlabeled}}$) in CO_2 respired by shoots (A) and roots (B) of perennial ryegrass during labeling. Each value is the mean of four to six replicate plants ($\pm 1\text{SE}$). Lines denote model predictions (Fig. II.4). Insets expand the first 48 h.

Compartmental model of substrate pools for respiration

The labeling kinetics reflected the operation of a substrate pool system supplying respiration. The structure of this system (number of pools, links between pools, delays, and sites of tracer entry and outlet) was determined by analysis of the tracer kinetics of respiratory CO_2 (Fig. II.3), including multi-exponential curve fitting to the tracer kinetics (similar to *e.g.* Moorby and Jarman, 1975), and consideration of established compartmental concepts of respiratory carbon metabolism (*e.g.* Farrar, 1990; Dewar et al., 1998), while respecting the (reductionist) principle of parsimony ('all other things being equal, the simplest solution is the best'):

- 1) The fast initial labeling of respired CO_2 [phase (i)] revealed a respiratory activity fed by a substrate pool very close to photosynthetic metabolism and hence rapidly renewed by assimilated tracer. This pool was named Q_1 and its respiratory activity F_{10} .
- 2) Further respiratory tracer release occurred only after a delay of several hours [phase (ii)], revealing the existence of a second respiratory activity (F_{20}) fed *via* another pool.
- 3) Fitting of a dual-exponential (instead of a mono-exponential) decay function to the tracer kinetics beyond 4 h of labeling increased the goodness of fit and gave a better distribution of residuals. More exponential terms, however, improved neither the fit nor the distribution of residuals. This indicated the existence of (at least) two additional respiratory substrate pools with distinct turnover times [phases (iii) and (iv)]. These pools were named Q_2 and Q_3 .
- 4) A small residual respiratory activity ($\sim 5\%$) [phase (v)] could not be characterized in terms of pool size and half-life because it released no tracer during the duration of

labeling.

- 5) The fact that pools Q_2 and Q_3 were resolved by respiratory tracer kinetics meant that respiratory activity F_{20} was fed *via* Q_2 , the faster of the two pools.
- 6) Of the several possibilities to arrange pool Q_3 in the model (*e.g.* by exchanging with Q_1 , Q_2 , or with both Q_1 and Q_2) we chose the simplest and biologically most meaningful: pool Q_3 supplied respiration by acting as a store, thus, by exchanging carbon with Q_2 .
- 7) The 0.8-h delay in labeling of respiratory CO_2 in roots relative to that in the shoot was interpreted as the time required for phloem transport of tracer from shoot to root.

A three-pool model with one delay was capable of accounting for all of the above-mentioned features of shoot respiration (Delay 1 in Fig. II.4). The same model with an additional (~ 0.8 h) delay for tracer release fitted root respiration (Delay 2). In this model – a map of respiratory carbon metabolism of the shoot and the root – carbon fixed in photosynthesis entered the respiratory system *via* Q_1 , where it was either respired or transferred to Q_2 . In Q_2 carbon was either respired directly or first cycled through Q_3 before being respired *via* Q_2 . This is not the simplest three-pool model (this would consist of three independent and isolated pools, each receiving tracer and each releasing CO_2), but it is the simplest with biological consistency able to reproduce the observed tracer kinetics. Additional pools were not supported by the number of exponential terms found, and different arrangements of pools and fluxes were not supported by goodness of fits (*e.g.* linking Q_3 to Q_1 instead of to Q_2).

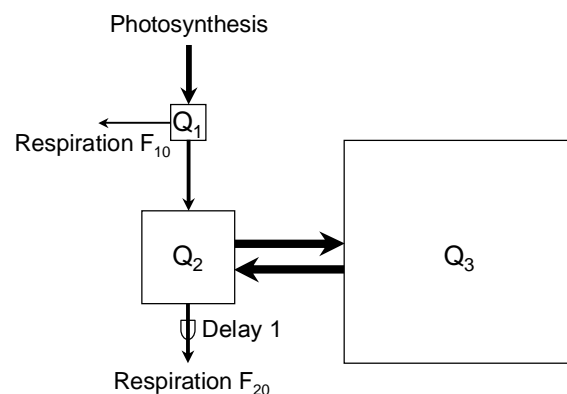


Figure II.4: Three-pool model of the substrate supply system of dark respiration of the shoot of perennial ryegrass. Carbon fixed in photosynthesis enters the respiratory system *via* pool Q_1 , where it is either respired (respiratory flux F_{10}) or transferred to pool Q_2 . In Q_2 carbon is either respired directly (F_{20}) or first cycles through Q_3 before being respired *via* Q_2 . Respiratory tracer release from Q_2 is associated with a delay. Functional characteristics of the pools (size, half-life and contribution to shoot and root respiration; Table II.1) were estimated by translating the model into a set of differential equations, and fitting the model to the tracer kinetics of shoot respiration. The same model also fitted the tracer kinetics of

dark respiration of the root, but included an additional delay of 0.8 h for tracer release in F_{10} and F_{20} . Arrows and boxes are scaled to indicate the magnitude of fluxes and pool sizes.

This model was translated into a set of differential equations (similar to Lattanzi et al., 2005) which described the system in terms of fluxes between pools and the environment, and implemented in a custom-made program using the free software ‘R’ (R Development Core Team, 2007). The program systematically tested millions of preset values for pool sizes, fluxes between pools and delays to find the lowest root mean squared error (RMSE). This extensive evaluation, first, assured that the absolute minimum RMSE was identified rather than a ‘local’ minimum, and second, revealed its sensitivity to changes in parameter values (Fig. II.5). These procedures were performed independently for the shoot and root data, thus generating independent estimates of system properties for the shoot and root.

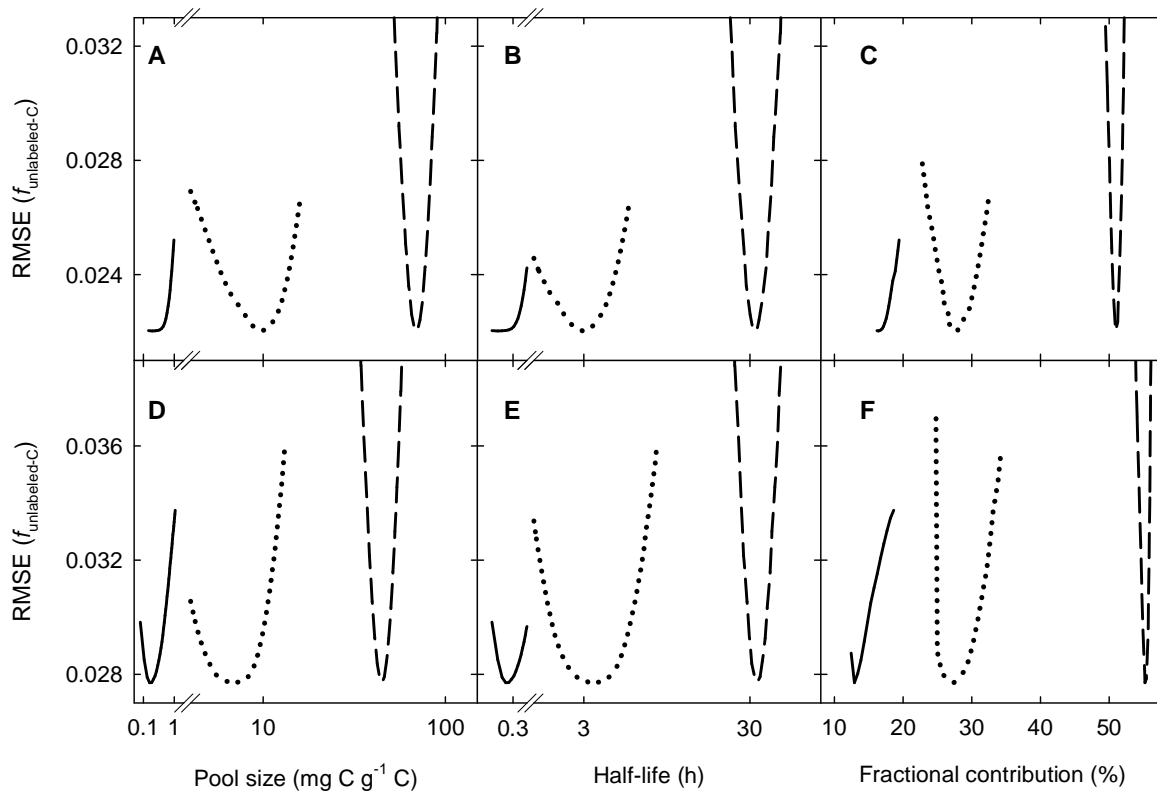


Figure II.5: Sensitivity of the goodness of model fits for the shoot (A-C) and the root (D-F) to departures from optimized values of pool size (A, D), half-life (B, E) and contribution to respiration (C, F). Sensitivity is expressed by the root mean squared error (RMSE) of the fit (minimum RMSE indicates the optimum value of a model parameter). The solid line represents Q_1 , the dotted line Q_2 , and the dashed line Q_3 . Note the logarithmic scaling of the x-axis for pool size and half-life.

Pool sizes, half-lives and contributions to respiration

Pool's half-lives were derived from fitted pool sizes and fluxes. The contribution of each pool to respiration was determined as the probability of carbon cycling through that pool before being respired. Pools Q_1 , Q_2 and Q_3 differed greatly in size and half-life (Table II.1). The relative sizes of the three pools were similar in the shoot and root, but root pools were 30 to 50% smaller than shoot pools because root respiration rate was half that of the shoot (Fig. II.2).

Table II.1: Optimization results for the parameters of the model shown in Figure II.4, as applied to the tracer time courses of shoot and root respiration (Fig. II.3). Model parameters include the size, half-life and percentage contribution to respiration of pools Q_1 , Q_2 and Q_3 . Together, the three pools accounted for 95% of shoot and root respiration. The remainder was supplied by sources which released no tracer within the 25 d-long labeling period (Fig. II.3). The quality of the fits is expressed as the root mean squared error (RMSE).

Pool	Shoot	Root
Size (mg C g ⁻¹ plant-C)		
Q_1	≤0.2	≤0.2
Q_2	9.7	6.9
Q_3	70.3	45.0
Half-life (h)		
Q_1	≤0.1	≤0.2
Q_2	2.9	3.4
Q_3	33.0	33.2
Contribution (%)		
Q_1	16	13
Q_2	28	27
Q_3	51	55
Delay 1 (h)		
—	3.7	4.1
Delay 2 (h)		
—	—	0.8
RMSE		
—	0.022	0.028

Q_1 was a very small, rapidly turned-over pool. Both in the shoot and in the root it was equivalent to 0.02% of total plant carbon, and its half-life was in the order of 0.1 to 0.2 h. Q_2 of the shoot represented ~1% and Q_2 of the root ~0.7% of total plant carbon, and both had a half-life of ~3 h (Table II.1). Q_3 was the largest: its shoot component comprised 7% and the root component 4.5% of total plant carbon. The half-life of Q_3 was virtually identical in both organs: 33 h. In total, 13.2% of all plant carbon formed part of respiratory substrate pools.

Although Q_1 was a very small pool, it served a significant role in respiration: 16% of shoot respired carbon and 13% of root respired carbon cycled only through Q_1 (Table II.1). The bulk, 79% of shoot respiration and 82% of root respiration, was supplied by Q_2 . Respiration *via* Q_2 was supplied by direct transfer of current photosynthate *via* Q_1 , and by carbon that first cycled through Q_3 (Fig. II.4). Direct transfer accounted for 28% of shoot respiration and 27% of root respiration. This meant that two pools whose carbon was renewed very rapidly by current photosynthetic assimilation supplied 44% of shoot respiration and 40% of root respiration. On the contrary, Q_3 , with a half-life of 33 h, played a (short-term) storage role and was the main source of substrates for respiration: 51% of all carbon respired in the shoot and 55% of that respired in the root cycled through this pool at least once before being respired (Table II.1). In both organs, 5% of respired carbon derived from a pool that could not be characterized in terms of size and half-life. Sensitivity analyses showed that estimates of pool's size, half-life and contributions to respiration were well constrained by the data (Fig. II.5).

DISCUSSION

The identity of respiratory substrate pools

This work indicates the existence of three pools supplying 95% of all substrate for respiration in intact plants of *L. perenne*. A most distinctive difference between these pools was the speed of carbon exchange by current assimilate: half-lives differed by almost four orders of magnitude between the fastest (Q_1) and the slowest pool (Q_3) (Table II.1, Fig. II.5). Each of these pools did likely not represent a single biochemical compound with a specific spatial location; rather they were probably mixtures of substrates distributed in different tissues and organs throughout the plant. Heterogeneous as they may be, these mixtures shared nonetheless a common pattern of tracer incorporation/release that compartmental analysis recognized. Hence, derived half-lives can be compared with known half-lives of putative substrates for respiration with the aim of attributing functional-biochemical identities to Q_1 , Q_2 and Q_3 .

Q_1 very quickly incorporated and released tracer. Thus, it was intimately connected with both CO_2 fixation and respiration. Its rapid turnover rate is consistent with the speed of labeling of primary photosynthetic products that are also involved in decarboxylation, including organic acids (Calvin and Bassham, 1964). Q_1 also contributed to root respiration, indicating a phloem-translocated component. Malate could have been a major constituent of Q_1 : it is rapidly labeled in leaves (Heber and Willenbrink, 1964), it is translocated to roots (Imsande and Touraine, 1994) and it is thought to be decarboxylated there (Imsande and Touraine, 1994; Stitt et al., 2002). Malate concentration is high in plants growing on nitrate (Leport et al., 1996), and may serve as a control and substrate for the nitrate uptake system (Imsande and Touraine, 1994). If this conclusion is true, then the relevance of Q_1 would depend on nitrogen source. We know of no other comparative studies of whole shoot and root respiratory tracer kinetics, which would allow an assessment of the generality of the present finding. Nogués et al. (2004) reported a rapid incorporation of tracer in CO_2 respired by *Phaseolus* leaves, consistent with tracer kinetics in Q_1 . But no study of tracer incorporation in root respiration has reported the existence of Q_1 . Perhaps, the participation of Q_1 in respiration is not a ubiquitous feature. An essential factor in identifying Q_1 was the existence of a few-hours lag between tracer incorporation and release from Q_2 (see below). Had there been no lag, then tracer release from Q_2 would have overlain that of Q_1 , rendering it unnoticeable.

The half-life of Q_2 (3 h) was close to, but longer than, the half-life often ascribed to a pool of 'transport sucrose' (1 to 2 h: Moorby and Jarman, 1975; Bell and Incoll, 1982; Farrar and Farrar, 1986). This pool is composed of sucrose in the cytoplasm, apoplast, and sieve tubes and companion cells of the phloem in actively photosynthesizing and exporting C3 leaves (Geiger et al., 1983). The present study derived respiratory pool kinetics from measurements at the scale of whole shoots and roots, that is, from tissues of very different developmental status: growing (sink), mature and senescing. We know of no studies of the kinetics of the transport pool in vegetative sink tissues. In the leaf growth zone of *Festuca arundinacea* the turnover rate of total tissue sucrose varied between <1 h and ~4 h, depending mainly on growth rate and related sucrose import and use (Schnyder and Nelson, 1987). Sucrose turnover in metabolically active sink tissue would, it seems, be similar to that in actively photosynthesizing leaves. Therefore, an interpretation of the half-life of 3 h of Q_2 is that it represents the (activity-weighted) mean of the kinetics of the transport pool extending over both source and sink tissues in the plant.

There was a substantial delay between tracer uptake and respiratory tracer release from Q_2 (Delay 1, Figs. II.3 and II.4, Table II.1). This effect was observed in both shoot and root,

and therefore must have been related to metabolism and not to transport. Results of others suggest some delay between the arrival of sucrose in sink tissue and its use in respiration: in a study with *Festuca arundinacea* Allard and Nelson (1991) found that 90% of the tracer imported into leaf growth zones was still present in the water soluble carbohydrates fraction at 2 h after labeling source leaves, and hardly any label was present in structural material. In the work of Kouchi et al. (1985) and Lötscher and Gayler (2005) respiratory tracer release from roots of legumes did not start until ~2 h or longer after the beginning of labeling. But Dilkes et al. (2004) observed a very rapid labeling of root exudates in wheat, and no evidence for a marked delay between tracer release via exudates and respiration. A similar lag was observed in other experiments with *L. perenne* growing with a limited supply of nitrogen (chapter III), showing that the present observation was not a singular result. We cannot rule out the possibility that growth in continuous light was a factor. However, we cannot envisage the physiological mechanism of such an effect.

The half-life of 33 h and the large size of Q_3 suggest a storage pool. Nonstructural carbohydrates are generally considered as the main source of respired carbon (ap Rees, 1980; Tcherkez et al., 2003) and some of them are used as temporary stores (Smith and Stitt, 2007). In C3 grasses, such as *L. perenne*, carbohydrate storage occurs mainly in vacuoles in the form of sucrose or fructan (Farrar and Farrar, 1986; Pollock and Cairns, 1991; Vijn and Smeekens, 1999). Starch was only a trace component of biomass in this study (<1% of plant dry wt, data not shown), but water-soluble carbohydrates were present at high concentration, particularly in the shoot. A storage pool with a half-life in the range of 12 h to 24 h is often found in C3 plants and ascribed to vacuolar sucrose (Moorby and Jarman, 1975; Bell and Incoll, 1982; Farrar and Farrar, 1986). The dynamics of fructan turnover are less clear. Its half-life was found to be in the range of 2 to 5 h in leaf blades of *Hordeum distichum* and two *Poa* species (Farrar, 1989; Borland and Farrar, 1988), and 14 to 18 h in leaf sheaths of *Poa* (similar to a 9 to 15 h half-life of vacuolar sucrose; Borland and Farrar, 1988). Fructan stored in wheat stems did not turnover during the storage phase (Winzeler et al., 1990).

Proteins constitute another large plant fraction which turnover is closely connected with respiratory pathways (Lea and Ireland, 1999). Half-lives of soluble proteins are in the order of 3.5 to 8 days (Simpson et al., 1981; Dungey and Davies, 1982), much longer than the half-life of Q_3 . This indicates that if proteins contributed to Q_3 then this contribution must have been relatively small. Forcing the model to split Q_3 into two storage pools gave tentative support to this conclusion as it yielded one pool with a half-life of 20 h contributing ~40% of total respiration and the other pool with a half-life of ~4 days contributing ~10% of total

respiration.

The size of the respiratory substrate pool system and carbon use efficiency

Collectively the respiratory substrate pool system comprised 13.2% of the total carbon mass of plants, and most of this (~87%) was contained in Q_3 , the storage pool. In comparison, water-soluble carbohydrates accounted for 28% of total plant carbon, meaning that it contained much more carbon than all respiratory pools combined. This is expected because stores supply not only respiration but also carbon skeletons for new biomass. Assuming that water-soluble carbohydrates were the exclusive substrate for respiration (thus neglecting any contribution of other putative substrates such as malate or proteins), then 47% of the water-soluble carbohydrate-C was allocated to respiratory CO_2 . In that case, the remainder (53%) must have been allocated to new (structural) biomass. This corresponds to a carbon use efficiency (CUE) of 53% for water-soluble carbohydrates. This is a conservative (*i.e.* low) estimate of the CUE of water-soluble carbohydrates, as it ignored possible contributions to respiration by other substrates. Yet, this efficiency is close to empirical and theoretical estimates of photosynthetic CUE in young herbaceous plants (van Iersel, 2003).

Are shoot and root respiration supplied by the same pools?

The most striking result of this work was the great similarity of root and shoot respiratory tracer kinetics (Fig. II.3). This meant that the same compartmental model fitted the root and shoot data equally well (Table II.1, Fig. II.5): number of pools, their half-lives and relative sizes and their relative contributions to respired carbon were practically the same in both organs. The only notable difference was that tracer appearance in root respiration was delayed by ~0.8 h (Delay 2, Table II.1), a time entirely in agreement with phloem-transport velocity (Windt et al., 2006). These features are consistent with a single three-pool system feeding shoot and root respiration.

If the supply system for root and shoot respiration consisted of only three pools, where were they located? Q_1 and Q_2 supplied respiration directly and were active in the root and shoot (Fig. II.4), so both must have had shoot and root compartments connected *via* the phloem. Conversely, a large part of Q_3 must have been located in the shoot. This is because the 'root component' of Q_3 would have been equivalent to >30% of the carbon mass of the root system (calculated by multiplying Q_3 root of 45 mg C g⁻¹ plant-C with the shoot to root ratio of 3.8, and dividing by the estimated CUE of 0.53) a value much greater than the total mass of non-structural carbon in the roots (WSC: 7.9% of root carbon, protein: 10% of root

carbon, estimated from nitrogen content and a 3.1 carbon to nitrogen ratio). So, only a fraction of the respiratory CO₂ of roots could have come from stores located in the root. Accordingly, most of the Q₃-derived respiratory CO₂ of roots must have come from the shoot store(s). Indeed, as is typical in grasses (Sullivan and Sprague, 1943; Davidson and Milthorpe, 1966a), the bulk of non-structural carbohydrates and protein (94% and 83% of plant total, respectively) were contained in the shoot.

The role of stores and current photosynthesis in supplying respiration

More than half of respired carbon cycled, at least once, through a storage pool before being respired. Clearly, stores were a central part of respiratory carbon metabolism. That a significant fraction of respiration is supplied by stores has been suggested before (Kouchi et al., 1985; Kouchi et al., 1986; Dilkes et al., 2004; Lötscher and Gayler, 2005), although the kinetic properties of pools were not determined in these studies, nor the localization and operating controls discussed. This study revealed that these carbon stores were quite short-lived, and therefore might have a limited capacity to sustain current carbon use rates over extended periods.

Yet, carbon stores used in respiration showed a longer half-life (this study) than those supplying leaf growth (Lattanzi et al., 2005). Thus, leaf growth seems to be much more dependent on continued assimilation of carbon, which agrees well with results on carbon allocation shortly after severe defoliation: most carbon used for leaf growth was new (Avice et al., 1996; Schnyder and de Visser, 1999) while that sustaining root respiration was largely old (Avice et al., 1996). Indeed, rapid and drastic decrease of root respiration following defoliation (Davidson and Milthorpe, 1966b), may be due to the fact that substrate for root respiration is essentially derived from current CO₂ fixation and stores in the shoot. Thus, the localization of most of the respiratory substrate in the shoot indicates that the control of root activity by the shoot would occur *via* the control of both current photosynthate- and storage-mobilization.

In conclusion, this work revealed a tight plant-level integration of respiratory substrate pools and fluxes. Incidentally, the results of this work suggest that the tracer kinetics of root respiration can be inferred from that of the shoot (which was near-identical to that of the root), which is useful information for partitioning of autotrophic and heterotrophic respiration in ecosystem-scale studies. Future work should address the possible variability and controls of substrate pool properties (half-life and size) and of their contributions to root and shoot respiration.

Chapter III: Nitrogen Deficiency Increases the Residence Time of Carbon in the Respiratory Supply System of Perennial Ryegrass and Reveals a Constitutive Role of Long-term Stores

ABSTRACT

Knowledge about the possible variability and controls of substrate pools for plant respiration is scarce. Here, we studied the effects of plants' nitrogen nutrition on the respiratory carbon supply system of *Lolium perenne* L.. Plants were grown in stands with two contrasting levels of nitrogen fertilization in continuous light and labeled with $^{13}\text{CO}_2/^{12}\text{CO}_2$ for intervals of 1 h to 696 h duration, followed by measurements of rates and isotopic signatures of shoot- and root-respired CO_2 at each labeling time. The tracer time courses of plant-respired CO_2 were calculated and analyzed with compartmental models. Although growth and respiration rates were affected strongly by nitrogen fertilizer supply, the same model explained the respiratory labeling kinetics equally well in both nitrogen treatments. In each case the model included three substrate pools which differed strongly in their rates of turnover. Together, the three pools accounted for 21.9% (low nitrogen) and 16.6% (high nitrogen) of total plant carbon. Thus, nitrogen limitation considerably increased the size of the respiratory substrate supply system. Moreover, nitrogen limitation greatly slowed the turnover (*i.e.* increased the half-life) of the two larger pools, and it strongly increased the contribution of long-term stores to substrate supply of respiration. Thus, nitrogen stress resulted in a longer mean residence time of carbon in the respiratory supply system: from 36 h in full nitrogen supply to almost 6 d under nitrogen limited conditions.

Introduction

Knowledge about the factors governing the residence time of respiratory carbon in plants is of fundamental importance to understand processes from plant allocation patterns to ecosystem carbon fluxes and even global carbon balance. In principle, the residence time of respiratory carbon is determined by the size of the respiratory supply system and by the flux through it, the respiration rate. The time lag between the photosynthetic assimilation of tracer and its occurrence in root- or ecosystem respiration is often consulted to assess the residence time of carbon, and this lag may vary by several orders of magnitude between plant functional groups (Ekblad and Högberg, 2001; Bowling et al., 2002; Johnson et al., 2002; Knohl et al., 2005; Carbone and Trumbore, 2007). However, respiration draws on carbon from both current photosynthetic activity (new carbon) and from stores (old carbon), which is commonly found among species (Ryle et al., 1976; Flanagan et al., 1996; Lötscher and Gayler, 2005; Carbone and Trumbore, 2007). Thus, the residence time of respiratory carbon in the plant depends also on the kinetic and functional characteristics of respiratory substrate pools and their contribution to respiration.

Recently, Lehmeier et al. (2008; in the following referred to as chapter II) described the respiratory carbon supply system of the shoot and root of a perennial grass, grown in a controlled and constant environment, to consist of three major substrate pools. Two small, rapidly turned over pools of current photosynthate provided fast routes for almost half of respired carbon to be released within half a day after photosynthetic assimilation. The other half was provided by a big short-term store with a half-life of more than one day (chapter II). Thus, carbon stores are an integral and important component of respiratory carbon metabolism, and hence, directly interacting with the provision and the use of assimilate. It might therefore be expected that the pattern of carbon allocation towards those functionally distinct respiratory substrate pools reflects the availability of external resources for the plant. It is not known, however, whether the concept of a three-pool respiratory carbon supply system holds true for a range of environmental conditions, nor how resource availability affects the residence time of respiratory carbon.

Nitrogen nutrition, in particular, may be assumed to affect all components determining the residence time of carbon in the respiratory supply system. The concentration of carbohydrates – considered as the major source of respired carbon (ap Rees, 1980; Tcherkez et al., 2003; chapter II) – usually increases with nitrogen limitation (Robson and Deacon, 1978; Evans, 1983; Lawlor et al., 1989; Morvan-Bertrand et al., 1999), thus potentially increasing the size of the respiratory supply system. On the other hand, the respiration rate

was often found to be positively correlated with nitrogen concentration in the biomass (Makino and Osmond, 1991; Reich et al., 2006). Therefore, a positive relationship between the speed of turnover of respiratory carbon and the nitrogen nutrition *via* its effect on the source/sink relationship seems intuitive.

Excess carbon brought about by nitrogen limitation, however, might be deposited in metabolically inert long-term stores, which do not participate in accommodating day-to-day fluctuations of carbon metabolism; such storage strategies are indeed commonly described in literature (Chapin et al., 1990). If this was true, then the turnover rates of those pools which are actually routing most of the carbon to the centers of respiration, would show a less pronounced response to nitrogen limitation.

Thus, the assessment of nitrogen effects on the kinetic properties of carbon pools supplying respiration may provide important information about the role of long-term stores of carbon. To this end, we followed the approach described in chapter II for a quantitative description of the effects of nitrogen nutrition on the respiratory carbon supply system. We grew plants of perennial ryegrass (*Lolium perenne*, cv. Acento) in a steady-state with either low or high supply of nitrogen. Plants were dynamically labeled with $^{13}\text{CO}_2/^{12}\text{CO}_2$ for periods ranging from 1 h to almost 1 month, followed by measurements of rates and isotopic signatures of respired CO_2 . The time course of tracer incorporation into respired CO_2 was evaluated in terms of the number and the characteristics of the substrate pools supplying carbon to respiration. This information was extracted with compartmental analysis, a mathematical tool that has often been applied to study carbon fluxes in source leaves (*e.g.* Moorby and Jarman, 1975) but which has only recently received attention in characterizing sink systems (Lattanzi et al., 2005; chapter II). Specifically, we addressed the questions whether the plants' nitrogen supply level affects (i) the number of respiratory substrate pools and the structure of the system, (ii) the pools' sizes, turnover rates and their contributions to respiration, as well as the residence time of carbon in the respiratory system, (iii) the carbon use efficiencies of substrates and (iv) the functional identity of pools, that is, in particular, whether long-term stores become an important source for respiratory carbon in nitrogen limited growth conditions.

Materials & Methods

Plant material and growth conditions

As described in chapter II, seeds of perennial ryegrass were sown individually in plastic pots filled with washed quartz sand and arranged in plastic containers at a density of 378 plants

m^{-2} . Two containers were placed in each of four growth chambers (Convion E15, Convion, Winnipeg, Canada). Plants were grown in continuous light, supplied by cool white fluorescent tubes. Irradiance was maintained at $275 \mu\text{mol m}^{-2} \text{s}^{-1}$ photosynthetic photon flux density at plant height. Temperature was held at $20 \text{ }^\circ\text{C}$, relative humidity near 85%. The stands of two chambers received a modified Hoagland solution by an automated irrigation system containing 1mM NO_3^- throughout the experiment (low nitrogen), while the other two stands always received a nutrient solution with 7.5 mM NO_3^- (high nitrogen). The composition of the nutrient solution was (1) for low nitrogen: 1 mM KNO_3 , 1 mM MgSO_4 , $0.18 \text{ mM KH}_2\text{PO}_4$, $0.21 \text{ mM K}_2\text{HPO}_4$, 0.5 mM NaCl , $0.7 \text{ mM K}_2\text{SO}_4$, 2 mM CaCl_2 ; micronutrients: $125 \mu\text{M Fe}$ -ethylenediaminetetraacetic acid, $46 \mu\text{M H}_3\text{BO}_3$, $9 \mu\text{M MnSO}_4$, $1 \mu\text{M ZnSO}_4$, $0.3 \mu\text{M CuSO}_4$, $0.1 \mu\text{M Na}_2\text{MoO}_4$; (2) for high nitrogen: $2.5 \text{ mM Ca(NO}_3)_2$, 2.5 mM KNO_3 , 1.0 mM MgSO_4 , $0.18 \text{ mM KH}_2\text{PO}_4$, $0.21 \text{ mM K}_2\text{HPO}_4$, 0.5 mM NaCl , 0.4 mM KCl , 0.4 mM CaCl_2 ; micronutrients were the same as in low nitrogen.

CO₂ control in the growth chambers and ¹³C labeling

Air supply to the four growth chambers was performed by mixing CO₂-free air and CO₂ with known carbon isotope composition (δ , with $\delta = [^{13}\text{C}/^{12}\text{C}_{\text{sample}} / ^{13}\text{C}/^{12}\text{C}_{\text{VPDB standard}}] - 1$). Within a nitrogen supply level, one chamber received ¹³C-depleted CO₂ ($\delta^{13}\text{C} -28.8\text{‰}$), while the other received ¹³C-enriched CO₂ ($\delta^{13}\text{C} -1.7\text{‰}$; both CO₂ from Linde AG, Höllriegelskreuth, Germany). Control was facilitated by measuring concentration and $\delta^{13}\text{C}$ of CO₂ entering and leaving each chamber online every 20-30 min by an infrared gas analyzer (IRGA, Li-6262, Li-Cor Inc., Lincoln, NE, USA) and a continuous-flow isotope-ratio mass spectrometer (CF-IRMS, Delta Plus, Finnigan MAT, Bremen, Germany). Both $\delta^{13}\text{C}$ and concentration of CO₂ ($360 \mu\text{L L}^{-1}$) inside the chambers were kept near constant by adjusting airflows and [CO₂] in the chamber inlets. For a more detailed description see Schnyder et al. (2003) and chapter II.

From three weeks after imbibition of seeds in high nitrogen supply, and from six weeks in low nitrogen, individual plants were labeled by swapping randomly selected plants between chambers (¹³C-enriched CO₂ → ¹³C-depleted CO₂ and *vice versa*). Since low nitrogen plants grew more slowly, the labeling of low nitrogen plants was delayed so that plants in both treatments were compared at a similar size. This aimed to minimize eventual size-related effects on the respiratory supply systems between treatments. Plants in high nitrogen were kept in the labeling chamber for 1, 2, 4, 8 or 16 h; or for 1, 2, 4, 8, 12, 17 or 25 d. The durations of labeling in the low-nitrogen treatment were 1, 2, 4, 8, or 16 h; or 1, 2, 4, 8 or 29 d. Labeling periods were scheduled in such a way that labeling duration and plant age at sampling were not strictly correlated.

Respiration measurements

Respiration of labeled plants as well as of non-labeled control plants was measured as described by Lötscher et al. (2004) and Klumpp et al. (2005). In brief, the system allowed the near simultaneous measurement of the rates of dark respiration as well as of the isotopic signatures of shoot- and root-respired CO₂ of individual plants. The system included four cuvettes, each for a single plant, which could be opened and closed quickly to insert a pot.

For measurements, plants were removed from the stands, installed in the cuvettes and kept in a growth cabinet held at the same temperature as the growth chambers. Every 45 min, three replicate measurements of CO₂, respired by shoots and roots of an individual plant were taken and dark respiration was recorded for ~5 h. Measurements of rates and $\delta^{13}\text{C}$ of shoot respiration reached a constant value by ~30 min after removing plants from the stands. However, it took ~1.5 h to purge the root-system free from extraneous CO₂ (*cf.* Lötscher et al., 2004). Each $\delta^{13}\text{C}$ sample was measured against a working standard gas which was previously calibrated against a VPDB-gauged laboratory CO₂ standard. The standard deviation of repeated single measurements was 0.08‰ for $\delta^{13}\text{C}$ and 0.33 $\mu\text{L L}^{-1}$ for the concentration of CO₂ on average of all measurements. During the 5 h measurements, dark respiration rates of roots decreased by about 3% and 6% for plants grown in low and high nitrogen supply, respectively, while that of shoots was constant during measurements in both treatments. Therefore, average rates served to calculate specific respiration rates. A detailed measurement protocol is given in chapter II.

Plant harvest and elemental analysis

Immediately after the termination of respiration measurements, plants were removed from the pots, washed free of sand, dissected into shoot and root, weighed, frozen in liquid nitrogen, and stored at -30 °C in chest freezers. All samples were freeze-dried for 72 h, weighed again, and ground to flour mesh quality in a ball mill. Aliquots of 0.75 mg \pm 0.05 mg of each sample were weighed into tin cups (IVA Analysentechnik e.K., Meerbusch, Germany) and combusted in an elemental analyzer (CarloErba NA 1110, CarloErba Instruments, Milan, Italy), interfaced to the CF-IRMS, to determine carbon and nitrogen contents.

Analysis of water-soluble carbohydrates

Water-soluble carbohydrates in plant biomass were analyzed similarly to the procedure described by Thome and Kühbauch (1985). In short, 60 and 80 mg of freeze-dried ground material of shoot and root samples, respectively, were weighed in Eppendorf tubes and

extracted with 2 mL H₂O for 10 min in a water bath at 93 °C. Afterwards, samples were cooled down and transferred to a rotating Heidolph shaker for 45 min at room temperature and then centrifuged by 10 000 rpm for 15 min. A 0.2 mL aliquot of the supernatant was transferred to a preparative HPLC system for separation of water-soluble carbohydrate fractions. Separation occurred in a Shodex KS 2002 (Showa Denko, Japan) chromatographic column held at a temperature of 50 °C and a system pressure of 17 bar and elution rate of 0.9 mL min⁻¹ using HPLC gradient grade (Baker, The Netherlands) as eluent. After 45 min, the samples had passed the HPLC-system and were immediately conveyed to a continuous-flow system. There, 1.25% (v/v) sulfuric acid was added to the samples at a rate of 0.9 mL min⁻¹, and di- and oligosaccharides were hydrolyzed to monosaccharides in a sample loop of 12.5 m length which was kept in a water bath at 95 °C. The samples arrived at a spectral photometer (K-2500/A4080, Knauer, Germany), which operated at wave length of 425 nm and quantified the carbohydrates by measuring the reducing power of the hydrolyzed carbohydrates with a potassium ferricyanide solution as described by Suzuki (1971). Analytical grade fructose (D(-)-Fructose, Merck, Germany) served as standard for carbohydrate quantification. The measurement cycle from start of HPLC-analysis to the colorimetric measurements took 110 min. The concentration of carbohydrate fractions on a plant level were calculated from the carbohydrate contents of shoot and root samples and the shoot- and root-mass fractions of the individual plants.

Data analysis

At a given labeling duration, the proportion of carbon in shoot- and root-respired CO₂ that was assimilated before (unlabeled) and during labeling, $f_{\text{unlabeled-C}}$ and $f_{\text{labeled-C}}$ (where $f_{\text{labeled-C}} = 1 - f_{\text{unlabeled-C}}$), was calculated as by Schnyder and de Visser (1999):

$$(1) \quad f_{\text{unlabeled-C}} = (\delta^{13}\text{C}_S - \delta^{13}\text{C}_{\text{new}}) / (\delta^{13}\text{C}_{\text{old}} - \delta^{13}\text{C}_{\text{new}}),$$

where $\delta^{13}\text{C}_S$, $\delta^{13}\text{C}_{\text{old}}$ and $\delta^{13}\text{C}_{\text{new}}$ are the $\delta^{13}\text{C}$ of respiratory CO₂ produced by the labeled sample plant, and non-labeled plants growing continuously in the chamber of origin ('old') or in the labeling chamber ('new'). $\delta^{13}\text{C}_S$, $\delta^{13}\text{C}_{\text{old}}$ and $\delta^{13}\text{C}_{\text{new}}$ of shoots were obtained as

$$(2) \quad \delta^{13}\text{C}_X = (\delta^{13}\text{C}_{\text{in}} F_{\text{in}} - \delta^{13}\text{C}_{\text{out}} F_{\text{out}}) / (F_{\text{in}} - F_{\text{out}}),$$

where X stands for 'sample', 'new' or 'old' (as appropriate), and $\delta^{13}\text{C}_{\text{in}}$, $\delta^{13}\text{C}_{\text{out}}$, F_{in} and F_{out}

are the isotopic signatures and the flow rates of the CO₂ entering and leaving the shoot compartment, respectively. Calculations for the root compartment were done in the same way in considering that the concentration and $\delta^{13}\text{C}$ of the CO₂ entering the root compartment was equal to that in the shoot compartment (*cf.* Klumpp et al., 2005).

It was shown for plants in high nitrogen supply, that the $\delta^{13}\text{C}$ of shoot-respired CO₂ of non-labeled control plants as well as that of labeled plants did not change during the respiration measurements (except in plants labeled for 1 h, which was accounted for in the calculations; see chapter II). The same was true for low-nitrogen plants, and from 1.5 h after transfer, the $\delta^{13}\text{C}$ of root respiration in both treatments was stable, too. Thus, $\delta^{13}\text{C}$ of respiratory CO₂ of the shoot or root of one plant were taken as the means of the measurements. The fraction of unlabeled carbon in CO₂ respired by a plant (Fig. III.3) was obtained as

$$(3) \quad f_{\text{unlabeled-C}} = (f_{\text{unlabeled-C shoot}} * R_{\text{shoot}} + f_{\text{unlabeled-C root}} * R_{\text{root}}) / (R_{\text{shoot}} + R_{\text{root}})$$

where R_{shoot} and R_{root} are the (absolute) respiration rates of shoot and root, respectively.

Compartmental analysis of tracer time courses in respired CO₂

The labeling kinetics of CO₂ respired by plants grown with either low or high level of nitrogen supply shows that tracer incorporation into respired CO₂ occurred in distinct phases (Fig. III.3), which reflected the operation of substrate pools supplying carbon to respiration. The structure of the systems (number of pools, links between pools, and sites of tracer entry and outlet) were determined by analyzing the tracer time courses with compartmental models as described in chapter II. This included (i) the fitting of exponential decay functions to the tracer kinetics to determine the number of mixing pools (similar to *e.g.* Moorby and Jarman, 1975) and (ii) the consideration of established compartmental concepts of respiratory carbon metabolism in arranging pool networks (*e.g.* Farrar, 1990; Dewar et al., 1998).

It is important to note, that the respiratory substrate pools are exclusively differentiated upon their functions as sources of respired carbon, exposed by their half-lives. That is, a pool may contain a variety of biochemical compounds, even compartmented in physical distinct tissue, which, however exhibit the same proportion of label with time, and are thus recognized by compartmental analysis as one individual pool (Atkins 1969, Jacquez, 1996; Rescigno 2001).

The analysis resulted in the three-pool model shown in Figure III.4 which, considering

the principle of parsimony, provided the best fits to the labeling kinetics. This model was translated into a set of equations, which described the respiratory supply system in terms of fluxes between pools and the environment under the assumptions, that pool sizes are steady, and that fluxes obey first-order kinetics. The fraction of tracer in each compartment with respect to time was given by:

$$(4a) \quad f_{\text{unlabeled-C-Q1}} = (Q_1 * f_{\text{unlabeled-C-Q1}} + F_{\text{In}} * f_{\text{labeled-C}} - F_{10} * f_{\text{unlabeled-C-Q1}} - F_{12} * f_{\text{unlabeled-C-Q1}}) / Q_1$$

$$(4b) \quad f_{\text{unlabeled-C-Q2}} = (Q_2 * f_{\text{unlabeled-C-Q2}} + F_{12} * f_{\text{unlabeled-C-Q1}} + F_{32} * f_{\text{unlabeled-C-Q3}} - F_{23} * f_{\text{unlabeled-C-Q2}} - F_{20} * f_{\text{unlabeled-C-Q2}}) / Q_2$$

$$(4c) \quad f_{\text{unlabeled-C-Q3}} = (Q_3 * f_{\text{unlabeled-C-Q3}} + F_{23} * f_{\text{unlabeled-C-Q2}} - F_{32} * f_{\text{unlabeled-C-Q3}}) / Q_3$$

$$(4d) \quad f_{\text{unlabeled-C}} = (F_{10} * f_{\text{unlabeled-C-Q1}} + F_{20} * f_{\text{unlabeled-C-Q2}}) / (F_{10} + F_{20}),$$

where Q_1 , Q_2 and Q_3 are pool sizes and F_{In} is the flux of assimilated carbon (tracer) that enters the respiratory system. The system is considered as steady and thus, F_{In} equals the specific respiration rate, $F_{\text{In}} = F_{\text{Out}}$, $F_{\text{Out}} = F_{10} + F_{20}$ (Fig. III.4), $F_{12} = F_{20}$ and $F_{23} = F_{32}$. Indices refer to donor and receptor pools, respectively. Index 0 represents the environment. The measured parameter against which the model prediction is compared is $f_{\text{unlabeled-C}}$. $f_{\text{unlabeled-C-Qi}}$ is the fraction of unlabeled carbon in a pool Q_i . $f_{\text{labeled-C}}$ is the constant fraction of fully labeled carbon entering the system after the start of labeling.

To account for the stable degrees of labeling from ~2-4 h (Fig. III.3), a delay was inserted in the model (Fig. III.4) by forcing $f_{\text{unlabeled-C-Q2}}$ in eqn. 4d to lag temporally behind $f_{\text{unlabeled-C-Qi}}$ in eqns. 4b and c for the numerical value of the delay. The delay only applied to tracer content in F_{20} , and had therefore no effect on the assessment of Q_2 and Q_3 half-lives.

The set of equations (4) was implemented in a custom-made program using the free software 'R' (R Development Core Team, 2007) with the aim of fitting the model to the tracer kinetics. Initial values for pool sizes, fluxes between pools and the delay were inserted, and the equations were solved. In that way, a tracer time course across the entire labeling period (696 h for low and 600 h for high nitrogen) was generated. The quality of the fit was expressed as the root mean squared error (RMSE).

This procedure was followed millions of times by stepwise and systematic variation of preset values for pool sizes, fluxes between the pools and the delay. In doing so, the combinations of pool sizes, fluxes and the delay which gave the best fits, i.e. the lowest RMSEs, were then taken as the ones closest to the real properties of the respiratory supply

systems. The extensive scanning procedure with numerous possible combinations further revealed the sensitivity of the fits to changes in parameter values (Fig. III.5).

Optimized pool sizes and fluxes served to calculate the half-life of a pool of size Q_i :

$$(5) \quad t_{1/2}(Q_i) = \ln(2) / (F_i / Q_i),$$

with F_i the sum of all fluxes leaving the pool Q_i .

Based upon optimized fluxes, the quantitative contribution of a pool Q_i (C_{Q_i}) to respiratory carbon release was derived, which is defined here as the probability of tracer moving in a certain flux of the respiratory system (*cf.* Fig. III.4):

$$(6a) \quad C_{Q_1} = F_{10} / (F_{10} + F_{12})$$

$$(6b) \quad C_{Q_2} = (1 - F_{10} / (F_{10} + F_{12})) * F_{20} / (F_{20} + F_{23})$$

$$(6c) \quad C_{Q_3} = (1 - F_{10} / (F_{10} + F_{12})) * F_{23} / (F_{20} + F_{23})$$

C_{Q_1} is the probability that tracer enters the system and leaves it in F_{10} without visiting any other pool. C_{Q_2} implies, that tracer enters Q_2 *via* Q_1 and is respired in F_{20} without moving through Q_3 . C_{Q_3} is the probability of tracer cycling through Q_3 at least once.

The mean residence time (MRT) of carbon in the respiratory supply system was calculated as the flux-weighted average of the half-lives of the three pools:

$$(7) \quad \text{MRT} = (t_{1/2} * C_{Q_1} + t_{1/2} * C_{Q_2} + t_{1/2} * C_{Q_3}) / \ln(2)$$

The analysis of tracer time courses conducted in the present study holds assumptions generally made in compartmental modeling, namely: (1) the system is steady, (2) fluxes obey first-order kinetics and (3) pools are homogeneous and well mixed. Support for the validity of assumption (1) is presented in the following section. Assumption (2) is probably false in a strict sense, but support for its practical validity has been found repeatedly (see Farrar, 1990 for a discussion). For a discussion of assumption (3) the reader is referred to chapter II, as the approach in the present chapter is carried out analogously.

Results

Rates of growth and respiration and photosynthetic carbon use efficiencies

The level of nitrogen supply had large effects on several plant growth parameters (Table III.1), but there were no differences between growth chambers within nitrogen supply levels, ($p > 0.05$; data not shown). During the experiment plants grew at constant specific rates (Fig. III.1). Linear regression of ln-transformed carbon mass data yielded average increments of $1.58 \text{ mg C g}^{-1} \text{ C h}^{-1}$ in low nitrogen supply, and $3.23 \text{ g C g}^{-1} \text{ C h}^{-1}$ at high nitrogen supply. So, the specific growth rate at high nitrogen was twice that at low nitrogen (Table III.1). Within one nitrogen treatment, specific growth rates of shoot and root were similar (chapter II; data for low nitrogen not shown). This resulted in near constant shoot to root ratios that averaged 3.0 and 3.8 $\text{g C g}^{-1} \text{ C}$ for plants in low and high nitrogen supply, respectively (Table III.1), in good agreement with generally observed effects of nutrient limitation on carbon allocation patterns (Mooney et al., 1995; Poorter and Nagel, 2000).

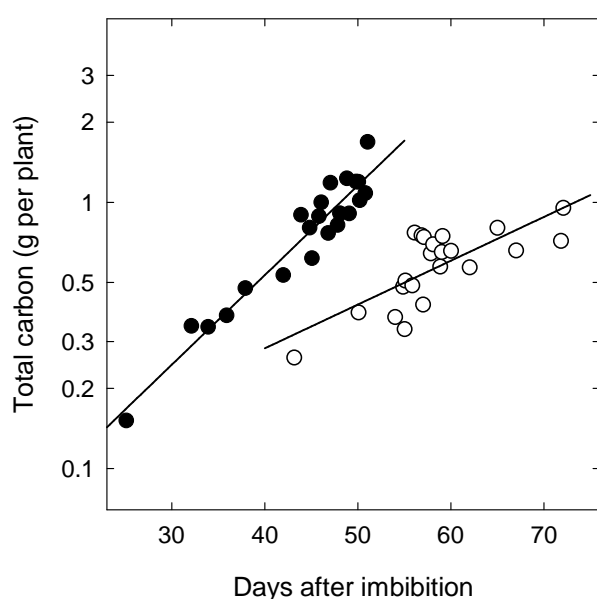


Figure III.1: Total carbon mass of perennial ryegrass grown with a nitrogen supply of either 1.0 mM (open symbols) or 7.5 mM (closed symbols). Each value is the mean of 3-6 replicate plants. Lines denote linear regression ($p < 0.05$; see also Table III.1). Note the logarithmic scaling of the y-axis.

Table III.1: Growth parameters of perennial ryegrass grown with either a low (1.0 mM) or a high (7.5 mM) supply of nitrogen. Values are means of 56 and 60 replicate plants for low and high nitrogen, respectively, $\pm 1\text{SE}$. Significant differences are based on a t-test, *** $P \leq 0.001$.

Parameter	Low nitrogen	High nitrogen	
Specific respiration rate, $\text{mg C g}^{-1} \text{ C h}^{-1}$	0.99 ± 0.03	1.50 ± 0.02	***
Specific growth rate, $\text{mg C g}^{-1} \text{ C h}^{-1}$	1.58 ± 0.31	3.23 ± 0.21	***
Specific Nitrogen uptake rate, $\text{mg N g}^{-1} \text{ N h}^{-1}$	1.16 ± 0.33	2.40 ± 0.20	***
Shoot : root ratio	2.96 ± 0.10	3.84 ± 0.14	***
C : N ratio (w/w)	48.8 ± 1.3	24.1 ± 0.5	***

The respiration rate is often found to be positively correlated with the nitrogen status of plants (Makino and Osmond, 1991; Reich et al., 2006). In accordance, the specific respiration rate of plants in high nitrogen supply was $1.50 \text{ mg C g}^{-1} \text{ C h}^{-1}$, about 50% higher than in low nitrogen ($0.99 \text{ mg C g}^{-1} \text{ C h}^{-1}$, Table III.1). This corresponded to photosynthetic carbon use efficiencies [CUEs, with $\text{CUE} = \text{growth rate} / (\text{growth rate} + \text{respiration rate})$] of 0.61 and 0.68 for plants in low and high nitrogen supply, which is well in the range of CUEs reported for young herbaceous plants (Gifford, 2003; van Iersel, 2003). In low nitrogen plants, the carbon to nitrogen ratio in biomass was twice as high (Table III.1) and their specific respiration per unit nitrogen was 30% higher rate than with high nitrogen supply (Fig. III.2). Rates in both treatments, however, were constant throughout the labeling period. Along with constant specific growth rates, this indicated that the systems were virtually in a steady-state. Thus, one basic assumption of compartmental analysis can be considered as met.

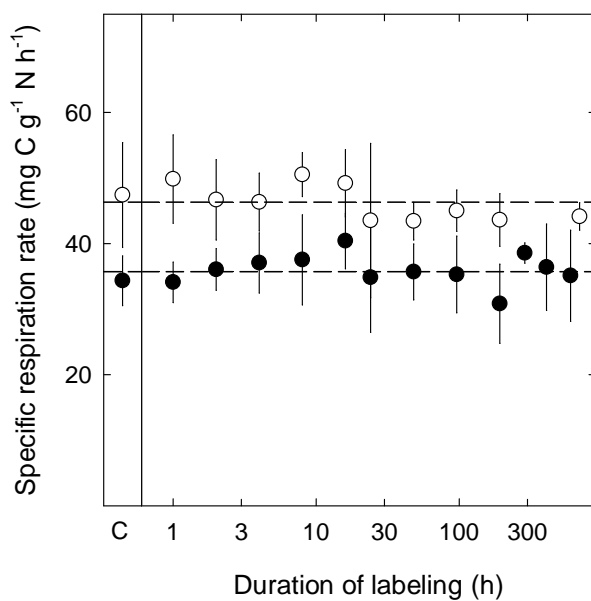


Figure III.2: Specific respiration rates of perennial ryegrass grown with a nitrogen supply of either 1.0 mM (open symbols) or 7.5 mM (closed symbols), labeled for different time intervals, and of non-labeled controls (C; at left). Each value is the mean of 3-12 replicate plants ($\pm 1\text{SE}$). Average rates were 46.3 ± 0.8 ($n=56$) and 35.7 ± 0.7 ($n=60$) for low- and high-nitrogen plants, respectively (dashed lines). Regression analysis yielded no significant trends ($p>0.05$). Note the logarithmic scaling of the x-axis.

Labeling kinetics of respired CO_2

The time courses of tracer incorporation into CO_2 , respired by plants of both nitrogen supply levels occurred in several distinct phases (Fig. III.3). In both nitrogen treatments, (i) a phase of a fast initial labeling was observed which was followed by (ii) a period where the degree of labeling remained constant. In that phase, respired CO_2 was more strongly labeled (+7%) in high nitrogen than in low nitrogen plants (0.84 vs $0.91 f_{\text{unlabeled-C}}$; Fig. III.3, inset). After 3-4 h, (iii) the fraction of unlabeled carbon decreased again in both treatments. It exhibited a faster rate of decrease in high nitrogen where this phase lasted until ~ 1 d of labeling, while it proceeded until ~ 2 -4 d in low nitrogen (Fig. III.3).

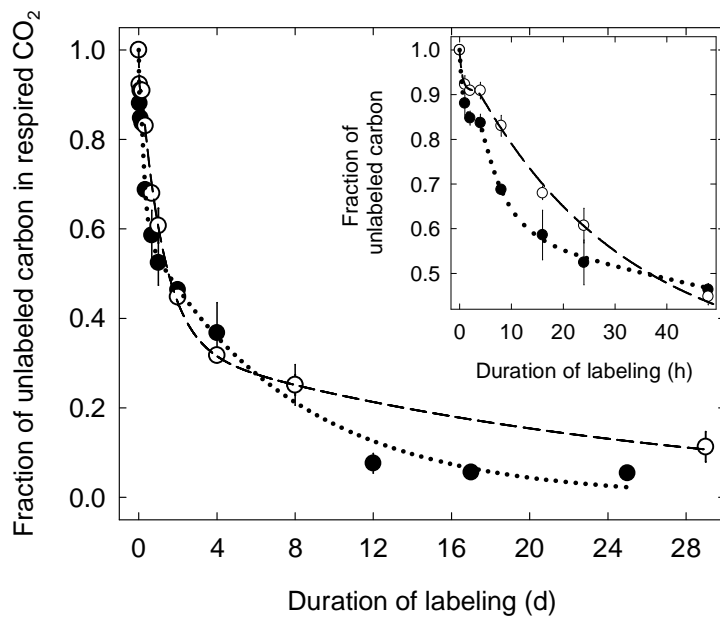


Figure III.3: Time course of tracer incorporation into CO_2 respired by perennial ryegrass plants grown with a nitrogen supply of either 1.0 mM (open symbols) or 7.5 mM (closed symbols) during labeling. Each value is the mean of 3-6 replicate plants ($\pm 1\text{SE}$). Lines denote model predictions (Fig. III.4). Inset expands the first 48 h. The data points at 8 d labeling duration overlap.

Thereafter, (iv) the fraction of unlabeled carbon in low nitrogen decreased at a very slow rate, and at 29 d, about 11% of respired carbon was still unlabeled. In high nitrogen supplied plants, the last phase exhibited a much faster rate of tracer incorporation and it was practically complete after 12 d, when the residual unlabelled respiratory activity had decreased to ~5% (Fig. III.3). The tracer kinetics in respiratory CO_2 of shoots and roots was very similar in low nitrogen (data not shown), the same as at high nitrogen (chapter II).

The respiratory carbon supply systems and substrate pool properties

Generally, tracer studies often aim at determining the number of pools involved in a certain process. Tracer appearance in different phases indicates the concerted involvement of distinct pools with different rates of turnover. In the present case, compartmental analysis revealed that the three-pool model shown in Figure III.4 adequately described the labeling kinetics of CO_2 respired by plants at both nitrogen supply levels (*cf.* RMSE, Table III.2). In both nitrogen treatments, a compartmental model with less than three pools was not able to adequately simulate the tracer kinetics as was evident from the quality of the fits and the distribution of residuals. On the contrary, four-pool models did not improve the fits, and – hence – would have caused over-parameterization of the model. So, the following (three-pool) compartmental model was defined: tracer fixed in photosynthesis entered the system *via* pool Q_1 , from which it was either respired directly *via* F_{10} or entered Q_2 . Once in Q_2 , carbon either cycled through pool Q_3 or left the system directly in the respiratory flux F_{20} without visiting Q_3 . In each nitrogen supply level, tracer appearance in F_{20} only occurred after a delay of 3-4 h after the onset of labeling (Fig. III.4, Table III.2).

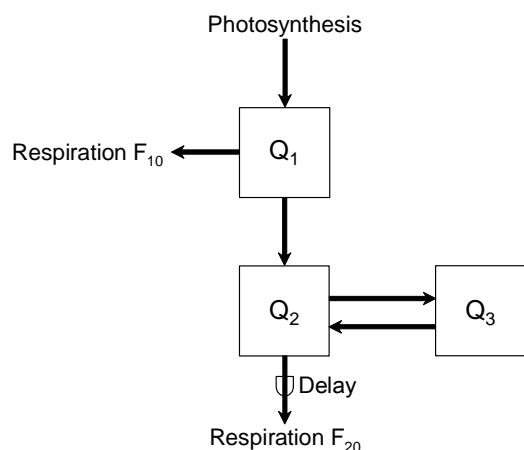


Figure III.4: Compartmental model of the three pools supplying carbon to respiration of intact perennial ryegrass plants. Tracer enters the plant during photosynthesis and is respired *via* Q_1 (F_{10}) or Q_2 (F_{20}). ‘Delay’ means a lag between tracer acquisition by Q_2 and its release in respiration. Functional characteristics of the pools (Table III.2) were estimated by translating the model into a set of differential equations, and fitting the model to the tracer kinetics.

This delay was observed in both shoot and root respiration in both nitrogen treatments (chapter II, no data shown for low nitrogen plants), and, therefore, was not related to long-distance transport. Accordingly, the delay must have been the consequence of some delay related to sink metabolism. The delay was well constrained by the data and it was very similar in both treatments. So, if it was influenced by nitrogen supply, the effect must have been small.

In both nitrogen treatments, the three pools differed greatly in size, half-life and contribution to respiration (Table III.2). Collectively they comprised 17% of the total carbon mass of plants at high nitrogen supply, and 22% at low nitrogen supply. Thus, nitrogen limitation caused a considerable increase in the relative size of the respiratory supply system. This increase derived mainly from large increases of pools Q_2 and Q_3 . Q_2 doubled in size with decreasing nitrogen supply, and Q_3 increased by about 20%. On the whole, Q_3 was by far the biggest pool, representing more than 80% of all respiratory carbon at both nitrogen supply levels. In both nitrogen treatments Q_1 was the smallest and fastest pool, showing a half-life of approximately 30 minutes. Due to its rapid turnover, the time resolution in the period of short labeling duration was not high enough to give more precise estimates of Q_1 half-lives. Thus, any eventual difference between treatments could not be detected. In contrast, the half-lives of the pools Q_2 and Q_3 were well constrained by the data and showed dramatic responses to nitrogen supply: the half-life of both pools increased by a factor of 6 with nitrogen limitation (Table III.2).

Table III.2: Optimized parameters (size, half-life and percentage contribution to respiration of pools Q_1 , Q_2 and Q_3) of the model shown in Figure III.4 fitted to tracer time-courses shown in Figure III.3. The quality of the fit is expressed as the root mean squared error (RMSE).

Pool	low nitrogen	high nitrogen
Size ($\text{mg C g}^{-1} \text{ plant-C}$)		
Q_1	1	1
Q_2	40	19
Q_3	178	146
Half-life (h)		
Q_1	0.4	0.5
Q_2	20	3.4
Q_3	263	40
Contribution (%)		
Q_1	9	15
Q_2	60	28
Q_3	31	57
Flux ($\text{mg C g}^{-1} \text{ plant-C h}^{-1}$)		
F_{10}	0.09	0.23
F_{12}, F_{20}	0.90	1.28
F_{23}, F_{32}	0.47	2.53
Delay (h)		
—	3.2	3.5
RMSE		
—	0.008	0.020

The labeling kinetics necessitated that respiratory CO_2 efflux preceded *via* two pools (see also chapter II). Despite its small size, Q_1 supplied a significant 15% of total respired carbon *via* F_{10} in high-nitrogen plants, while this proportion was only 9% in low nitrogen (Table III.2, see phase (ii), Fig. III.3, inset). The major part of respiration was supplied *via* F_{20} in both treatments. This flux included both the part of photosynthate passing directly through Q_2 [*cf.* phase (iii)], and carbon which cycled through Q_3 [*cf.* phase (iv)]. In high nitrogen supply, the direct transfer component accounted for 28% of respiration, while 57% of respired carbon had first cycled through Q_3 . This ratio was effectively reversed in plants with low nitrogen supply, as the contribution of Q_3 decreased to 31% while the direct transfer component actually

doubled to 60% (Table III.2). The increase in size of Q_3 , but mainly the dramatic decrease in the flux of carbon through Q_3 caused a substantial increase of the mean residence time of carbon in the respiratory supply system: calculated *via* the flux-(*i.e.* contribution)-weighted average of the three pools' half-lives the mean residence time was 36 h at high nitrogen and 135 h at low nitrogen.

Concentration and carbon use efficiency of water-soluble carbohydrates

Collectively, water-soluble carbohydrates accounted for $370 \text{ mg C g}^{-1} \text{ plant-C}$ in low nitrogen supply, almost 30% more than in high nitrogen (Table III.3). This difference was essentially due to the higher concentration of fructans in low nitrogen plants. In both treatments fructans accounted for the largest fraction of water-soluble carbohydrates. By contrast, the concentrations of glucose and fructose were lower in low nitrogen, while no difference in sucrose concentration was observed between treatments (Table III.3). Regardless of the nitrogen supply level, sucrose and hexoses together only accounted for 4% of total plant carbon.

The carbon use efficiency of carbohydrates was calculated as $\text{CUE} = 1 - (\text{size of the respiratory substrate pools} / \text{total water-soluble carbohydrate content})$ in assuming that carbohydrates were the only substrate for respiration. CUE was 0.41 in low nitrogen and 0.43 in high nitrogen plants. The value of 0.43 for high nitrogen plants is a little lower than that reported in chapter II, since there, the asymptotic 5% of tracer time course (Fig. III.3) was neglected in the estimation of respiratory substrate pool sizes.

Table III.3: Content of water-soluble carbohydrate fractions of perennial ryegrass grown with either a low (1.0 mM) or a high (7.5 mM) supply of nitrogen. Values are means of six replicate plants \pm 1SE, along with the significance of the difference based on a t-test. * $P \leq 0.05$; NS, not significant, $P > 0.05$.

	Low nitrogen	High nitrogen	
	$\text{mg C g}^{-1} \text{ plant-C}$		
Fructan	331 ± 22	242 ± 20	*
Sucrose	21 ± 1	23 ± 1	NS
Glucose	7 ± 0.3	11 ± 1	*
Fructose	11 ± 1	14 ± 1	*

Discussion

The same model describes the respiratory supply systems of both nitrogen treatments

The present work characterizes the effects of nitrogen availability on the respiratory carbon supply system of perennial ryegrass growing in a steady-state. Both with low and with high nitrogen supply, it was apparent that three major substrate pools provided carbon to plant respiration. Moreover, since the distinct phases of tracer incorporation into plant-respired CO_2 were qualitatively very similar in the two treatments (Fig. III.3), the same three-pool model (Fig. III.4) predicted both data sets equally well. In both cases it was the simplest model with biological consistency that accounted for all of the observed features of the respiratory ^{13}C tracer kinetics. This model included all essential and no redundant elements of the respiratory supply system making it a useful tool for investigations of the control of respiratory substrate metabolism by biotic and abiotic factors. This was also manifest in the sensitivity analysis of pool parameters which showed that the effect of nitrogen on respiratory system features were well constrained by the data (Fig. III.5), clearly differentiating features that were affected from those that were not affected by nitrogen nutrition.

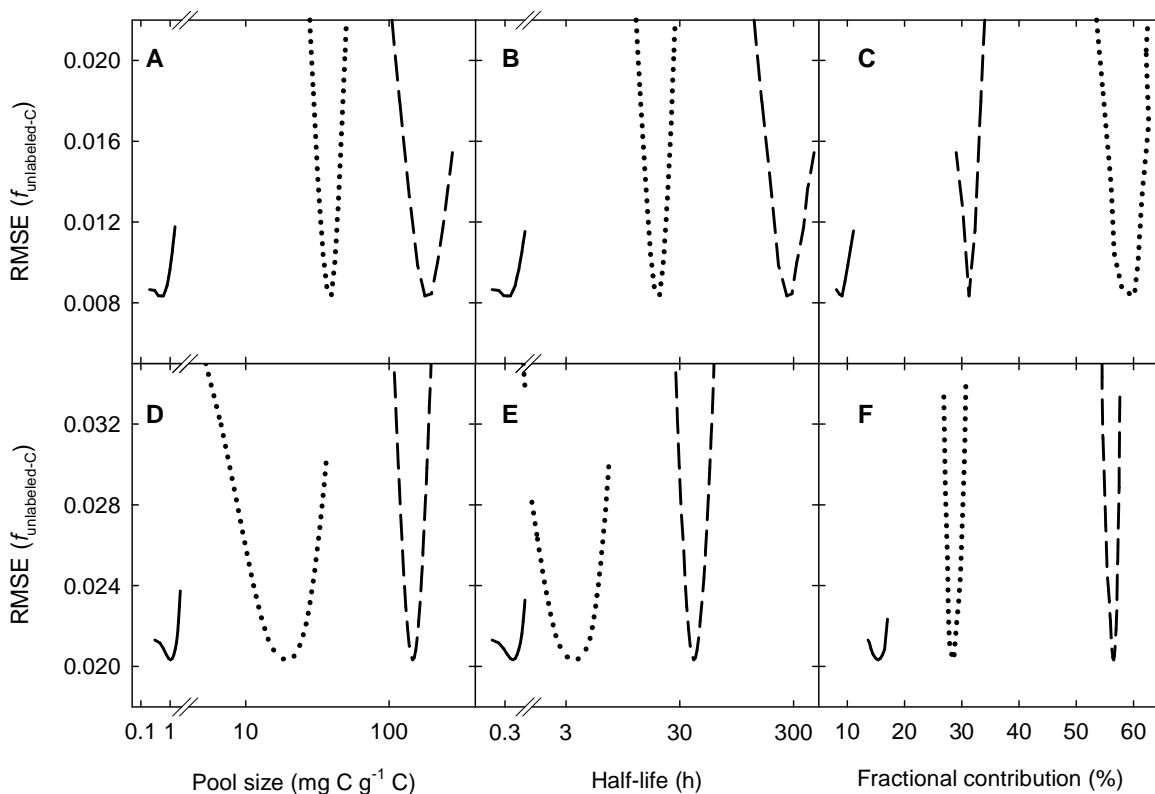


Figure III.5: Sensitivity of the quality of model fits for plants grown with a supply of either 1.0 mM nitrogen (A-C) or 7.5 mM (D-F) to variation of the optimized values of pool size (A, D), half-life (B, E) and contribution to respiration (C, F). Sensitivity is expressed by the root mean squared error (RMSE) of the fit (minimum RMSE indicates the optimum value of

a model parameter). The solid line represents Q_1 , the dotted line Q_2 , and the dashed line Q_3 . Note the logarithmic scaling of the x-axis for pool-size and half-life.

The functional identity of respiratory substrate pools

In both low and high nitrogen supply, Q_1 was the smallest and (with $t_{1/2} \approx 30$ min) the most rapidly turned over pool (Table III.2). Such a pool, having a half-life of ≤ 15 min, was shown to supply respiration of shoots and – with a 1 h delay due to phloem transport – the roots in high nitrogen plants (chapter II). The same was true for plants in nitrogen limitation (data not shown). Since the fractions of unlabeled carbon in plant-respired CO_2 were obtained by a flux-weighted average of shoot and root respiration, *i.e.* not differentiating for transport, the half-lives of Q_1 in both treatments were a little longer than those assessed at the shoot and root level.

The contribution of Q_1 increased with high nitrogen supply (Table III.2), and with a much higher respiration rate of those plants, the respiratory efflux F_{10} more than doubled (Fig. III.4, Tables III.1 and III.2). These results agree with the notion that this pool contains organic acids involved in nitrate uptake (chapter II), as nitrate uptake rates were much lower in nitrogen deficient plants (Table III.1). The conclusion, that organic acids become a quantitatively more important carbon source in respiration with nitrogen supply level, is supported by findings that the respiratory quotient may rise above unity with nitrate supply (Bloom et al., 1989; Bloom et al., 1992), a value that suggests substantial decarboxylation of organic acids.

The pool Q_2 exhibited a central function in the respiratory supply system, as it served as carbon source for the storage pool Q_3 and it was the main site of respiratory activity (F_{20} , Fig. III.4, Table III.2). Q_2 characteristics, however, responded so strongly to nitrogen supply level, that one must wonder, if this pool actually had the same physical/chemical identity in both nitrogen treatments. In high-nitrogen plants, the half-life of 3.4 h for Q_2 (Table III.2) is close to half-lives often attributed to the pool of ‘transport’ sucrose (Bell and Incoll, 1982; Farrar and Farrar, 1986). A comparison of Q_2 size and the concentration of sucrose in plant biomass (Tables III.2 and III.3) supports the opinion that Q_2 in high nitrogen supplied plants mainly contained ‘transport’ sucrose. But, in nitrogen limited plants, the size of Q_2 was larger than the total quantity of sucrose (Tables III.2 and III.3), demonstrating that it must have included a further component. Considering the notion of carbohydrates as the major source of respired carbon (ap Rees, 1980; Tcherkez et al., 2003), Q_2 in low nitrogen plants probably included a fructan component. Fructans are the main form of carbohydrate storage in vegetative plant parts of cool-season C3 grasses, such as *L. perenne*, and their storage occurs

in vacuoles (Pollock and Cairns, 1991; Vijn and Smeekens, 1999). Possibly, at low nitrogen, Q_2 represented a flux-weighted mean of respiratory activities from two sub-pools with transport and short-term storage functions which had turnover characteristics that were too similar to be resolved by tracer kinetics. With the present data alone, it is not possible to estimate how much each of those putative components contributed to Q_2 . But the half-life of 20 h for Q_2 at low nitrogen (Table III.2) suggests that the storage component was probably substantial.

Delivering 57% of plant-respired carbon, the storage pool Q_3 was the major source for respiration in high nitrogen supplied plants, and its half-life of 40 h demonstrated that it operated as a short-term store (Table III.2). This functional component presumably corresponds to the vacuolar carbohydrate storage component of Q_2 in nitrogen limited plants. Thus, Q_2 in low nitrogen may have been functionally equivalent to Q_2 plus Q_3 in high nitrogen plants. Considering the fact that Q_2 in low nitrogen supplied 60% of respired carbon (including carbon from both transport and short-term storage component), short-term stores must have become less important with nitrogen limitation. In these plants, however, Q_3 functioned as a long-term store and provided 30% of plant-respired carbon (Table III.2), while a distinct pool with the same functional identity was apparently absent in plants with full nitrogen supply.

The half-life of Q_3 of 263 h in nitrogen limited plants (Table III.2) appears far too long for a pool in leaf blade vacuoles (Farrar, 1989). Leaf sheaths are generally considered as a site of long-term carbon storage in grasses, and may become especially important in conditions when carbon supply by photosynthesis exceeds the sink demands (Pollock and Cairns, 1991). This was perhaps the case for plants in nitrogen limitation, as was indicated by the increase of the water-soluble carbohydrate concentration of $80 \text{ mg C g}^{-1} \text{ C}$ relative to high nitrogen plants (Table III.3). Following the notion of carbohydrates being the main source of respired carbon, then about two-thirds of this increase must have been allocated to the respiratory supply system, whose size increased by $53 \text{ mg C g}^{-1} \text{ C}$ with nitrogen limitation (Table III.2). Thus, the present results indicate that long-term stores became an integral part of plants respiratory carbon metabolism and an important source of respired carbon in nitrogen limited growth conditions. Interestingly, long-term stores of carbohydrates contributed very little substrate for leaf growth at both nitrogen supply levels (Wild et al., unpublished results). This suggests that, at least in conditions of nitrogen limitation, growth and respiration may draw on different substrate pools.

The size of the respiratory supply systems and carbon use efficiencies

The present compartmental model describes a *sink* system that comprises all the metabolic carbon in the plant that is eventually lost in respiration. In high nitrogen plants, the size of this system, *i.e.* the sum of the three pools, was equivalent to 166 mg C g⁻¹ plant C. With nitrogen limitation, the size of this system increased by 30% (Table III.2). Assuming, that the bulk of respiratory substrate pools – particularly Q₂ and Q₃ – was made up of carbohydrates, then 59% and 57% of the total water-soluble carbohydrates were allocated to respiration in low and high nitrogen supplied plants, respectively. Neglecting other sinks like exudation, the remainder was allocated to new structural biomass or (long-term) storage yielding a CUE of water-soluble carbohydrates of 0.41 and 0.43 at low and high nitrogen, respectively. Thus, despite of the fact that the nitrogen supply level had dramatic effects on the speed of storage turnover and the pattern of short- and long-term storage use (Table III.2), it had only little influence on the carbon use efficiency of water-soluble carbohydrates in total.

The CUE of carbohydrates is considerably lower than the photosynthetic CUE of >0.6 estimated by growth analysis. The reasons for this discrepancy could be manifold, but it may indicate that the conversion efficiency of current assimilation products into substrate for growth was much higher than the photosynthetic CUEs so that the lower values of CUEs of carbohydrates were compensated for. Possibly, the discrepancy could be due to a high efficient use of amino-C as substrate for growth.

The mean residence time of respiratory carbon

The most distinctive difference between treatments was the increase of the mean residence time of carbon in the respiratory supply system from 1.5 d to almost 6 d with nitrogen limitation. This was partially caused by the effect of nitrogen on the physical determinants of the residence time: the size of the system increased by 32%, and the respiration rate decreased by 30% (Tables III.1 and III.2). Assuming first-order system kinetics, these factors explain approximately a doubling of the mean residence time, which is only about half of the 4-fold increase of mean residence time that was actually observed. The remaining – and actually the most important – effect on the mean residence time came from the shifts in the contributions of functionally distinct substrate pools (Table III.2).

To our knowledge, effects of nitrogen on the mean residence time of respiratory substrate have not been shown before, minimizing opportunities for discussion. However, the finding that the fraction of old carbon in CO₂ dark-respired by roots was higher with nitrogen limitation after labeling for one photoperiod, has led to suggestion that the use of stores in

root respiration depended on plants' nitrogen availability (Hansen et al., 1992; Lötscher and Gayler, 2005). But other studies reported no detectable effect (Kouchi et al., 1986). The present study, conducted almost to isotopic equilibrium of the total respiratory supply system (Fig. III.3), revealed that the fraction of unlabeled carbon was initially higher in low nitrogen (from 1 to 24 h), then quite similar between treatments (from 1 to 2 d), then briefly higher in high nitrogen (around 4 d), to be finally higher again in low nitrogen (from 8 d till the end of the experiment). Thus, the time to exchange half the respiratory supply system was the same in both nitrogen supply levels: 35 h (Fig. III.3, inset). The analysis of tracer time courses with compartmental models, however, revealed that the effect of nitrogen on the residence time was due to the fact that a long-term storage pool with slow turnover provided significant amounts of carbon in low nitrogen, whereas this pool was absent in high nitrogen supplied plants.

This situation may occur frequently in natural and semi-natural ecosystems (like managed grassland), where nitrogen limitation is rather the norm than the exception (Afzal and Adams, 1992; Bogaert et al., 2000). The isotopic composition of ecosystem respiratory CO₂ is often taken as an indicator of ecosystem functioning (*e.g.* Flanagan et al., 1996; Buchmann and Ehleringer, 1998; Ekblad and Högberg, 2001). The present results show, that when using this approach, especially the dynamics of storage pools needs to be taken into account. That the nutrient status of plants exerts an influence on the residence time of respiratory carbon in plants (and hence, in ecosystems) has not been shown before and merits further examination.

Conclusions

The residence time of respiratory carbon is tightly linked to plants' nitrogen status and mainly controlled via deposition and mobilization fluxes involving short- and long-term storage components. The concept of a three-pool respiratory carbon supply system for grasses, however, was confirmed for widely contrasting availabilities of nitrogen to plants. Thus, the presented model may serve as a hypothesis for studies of respiratory carbon metabolism of plants with different strategies of carbon storage growing in contrasting environments.

Chapter IV: General and Summarizing Discussion

This work presents a comprehensive description of the respiratory carbon supply system of intact plants of perennial ryegrass. It is based on the kinetic characterization of the major respiratory substrate pools, what allowed to ascribe them a functional-biochemical identity, and their identification included three essential steps: (1) the steady-state of plant growth, (2) the dynamic $^{13}\text{CO}_2/^{12}\text{CO}_2$ labeling followed by direct measurements of respired CO_2 and (3) the analysis of tracer time courses with compartmental models.

Dynamic Labeling, Compartmental Models and Sensitivity Analysis

One major advantage of the present approach is that plants were grown in controlled and constant environments, with a constant isotopic composition of the source CO_2 . This was provided by controlling CO_2 in the chamber outlets (Fig. IV.1) and adjusting both CO_2 concentration and air flow at the chamber inlet (see Schnyder et al., 2003). Fluctuations in the signature of the photosynthetic flux due to, for instance, diurnal changes in water vapor pressure deficit or irradiance, which must be coped with in studies in natural environments, were obviated. Respiration measurements of non-labeled control plants which grew in isotopic equilibrium therefore provided the exact isotopic signatures of the two end members of the mixing model, *i.e.* of 100% old and 100% new carbon. Thus, the fraction of tracer in respired CO_2 at each labeling interval could be assessed very accurately (eqs 1, chapters II and III).

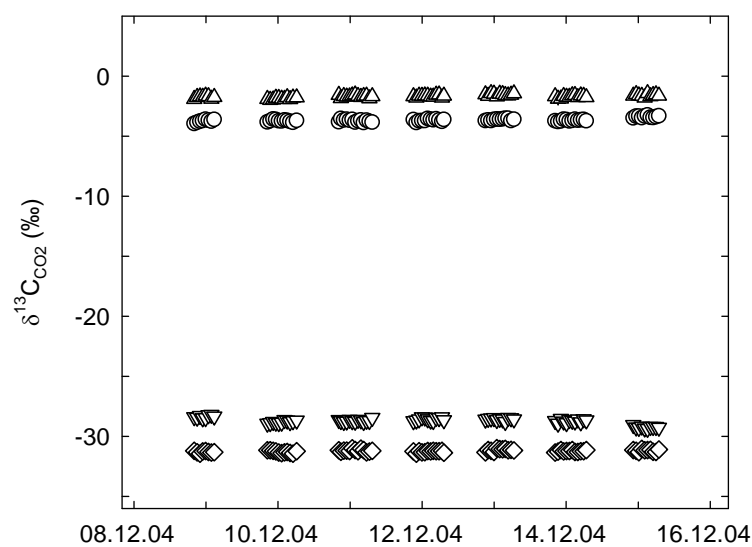


Fig. IV.1: C isotope composition (δ) of CO_2 leaving the four growth chambers during one week of the experimental period. Values are hourly means of four measurements of individual chambers with stands of 6-week-old (upright and downright triangles) and 10-week-old (circles and diamonds) perennial ryegrass plants grown in either low or high supply of nitrogen, respectively. The standard deviation of the means never exceeds the symbols' size.

The large differences in the isotopic composition of the source CO₂ of about 27‰ within one nitrogen treatment (Fig. IV.1) was much larger than the uncertainty (precision) of CO₂ measurements of ~0.10‰ (1 SD). This allowed the detection of minute amounts of tracer in respired CO₂, which proved to be essential for the assessment of system dynamics particularly in short-term labeling periods (Figs. II.3 and III.3). Also, carbon isotope discrimination ($\Delta^{13}\text{C}$) of plants grown in chambers with the same level of nitrogen supply but different source CO₂ was very similar (see chapter II; for low nitrogen data not shown). As $\Delta^{13}\text{C}$ is very sensitive to growth conditions, this indicated that growth in the two corresponding chambers occurred under virtually identical conditions, another prerequisite of the present approach.

The same or similar approaches of dynamic labeling with the aim to characterize respiratory substrate pools by direct measurements of respired CO₂ have been repeatedly used before. Usually, however, the labeling times have been much shorter than in the present study, reaching only about 50% label saturation in respired CO₂ (Kouchi et al., 1985, 1986; Schnyder et al. 2003, Nogués et al., 2004; Lötscher and Gayler, 2005). Labeling almost to (new) isotopic equilibrium allowed for the first time not only the determination of the number and kinetics of respiratory substrate pools, but actually the evaluation of the pool network and the quantification of carbon fluxes within the system and between the system and the environment, based on firm empirical evidence. The availability of a large number of individual plants in the present study ensured that dynamic labeling could be conducted with high temporal resolution, which is of special importance when dealing with pools having high turnover rates. Measuring 3-6 replicate plants per labeling interval provided representativeness of the data (Figs. II.3 and III.3).

The successful application of compartmental analysis to a tracer time course requires background knowledge about the biological processes and the structure of the real system under consideration (Jacques, 1996). Indeed, there is profound knowledge about respiratory carbon metabolism at the biochemical level, but there is still only fragmented information about the characteristics of the respiratory supply system at the level of organs or whole plants (ap Rees, 1980; Farrar, 1985). This suggested a very conservative use of compartmental analysis in the present study. We recognized, however, that commercial modeling software was of limited explanatory power for this purpose. Although such software provided a comprehensive description of the model which gave the absolute best fit, it was not discernable, how superior this solution was compared to others. That is, we could not answer the question, if the tracer kinetics could be predicted with one or even more other combinations of pool sizes and fluxes with almost the same statistical power. To address this

problem, we built the custom-made program described in chapter II to gain more insight in the optimization process. This procedure not only revealed the ‘best’ model, but in addition it demonstrated the responses of the fit to changes in system parameters (Figs. II.5 and III.5). This sensitivity analysis not only compensated for error specification of pool properties, but it also detected redundant model parameters that were not supported by the data and thus, facilitated following the principle of parsimony in a rigorous manner.

The reductionist approach allowed a straightforward functional differentiation of the respiratory substrate pools and has, to our knowledge, not been used before. In principle, it may serve to analyze tracer time courses of any compartmental system, and it has already been successfully applied to infer the substrate supply system of leaf growth (Wild et al., unpublished results).

The Steady-State of Plant Growth

The analysis of tracer time courses with compartmental models holds the basic assumption that the observed system is in a steady state. That is, for an unbiased pool description, the system properties must not change with time except for tracer content. This aspect was assumed to be met in the present study, but merits further considerations.

Plant growth in continuous light aimed at achieving a steady-state in the short-term. In a natural light regime, storage pools are filled in light and depleted in the dark period (Farrar and Farrar, 1986; Gibon et al., 2004). Such fluctuations may not be critical for the steady-state assumption if the pool systems’ kinetics is described on a day-by-day basis (see Lattanzi et al., 2005). However, in the present study, a specific pool could be considered to have the same filling level at the end of each labeling time in terms of total specific carbon, which allowed the functional identification unaffected by pool size changes.

The respiration rates of shoot and root include respiration associated with growth (*e.g.* for the synthesis of shoot and root structural material or for nitrate uptake) and maintenance components (*e.g.* for protein turnover; Amthor, 2000; Cannell and Thornley, 2000). Their relative contributions to total respiration are known to change with the growth rate of plants (Van Iersel, 2003), and recent work suggests that growth respiration rather draws on products of current photosynthesis, while maintenance respiration seems to rely more on old carbon (Löttscher et al., 2004). Thus, a change in growth rate could trigger a change in the contribution of current photosynthate and stores *via* a change in the relative contribution of growth and maintenance respiration to total respiration. However, the constant specific growth rates (Fig. III.1) indicate that the functional requirements of the (vegetative) plants

and, consequently, the relative contributions of the respiratory substrate pools (Tables II.1 and III.2) were practically steady throughout the experiment. Furthermore, since each of the above mentioned processes are associated with particular costs of carbon (Penning De Vries et al., 1974; Penning De Vries, 1975; McDermitt and Loomis, 1981; Johnson, 1990), the constant specific respiration rates (Figs. II.2 and III.2) support the steady-state of the respiratory supply system.

One of the most significant findings of the present work is that shoot and root respiration were supplied by the same substrate pools, and a large part of respiratory carbon must have been residing in shoot tissue. This was based on the analysis of tracer time courses of plants grown in high nitrogen supply level (chapter II), but the same analysis of shoot- and root-kinetics of plants grown with low nitrogen supply yielded essentially the same conclusion (data not shown). Thus, it seemed that root respiration directly drew on the carbon which was supplied *via* the continuous delivery by phloem transport, and therefore the labeling kinetics of root-respired CO₂ largely reflected the allocation patterns between shoot pools. Supposedly, the continuity of this dynamic system behavior was supported by the constant supply of light and other factors such as the undisturbed growth of the plants.

Non-Steady-State Plant Growth

It might be questioned, if the tight plant-level integration of respiratory carbon pools and fluxes observed in steady-state conditions would also hold true for systems in non-steady-state. Indeed, in other experiments (not presented here) we have obtained experimental evidence (Fig. IV.2) that massive disturbance, in this case defoliation, actually disrupted the shoot-root integration of respiratory substrate pools, demonstrated by the divergence of the labeling kinetics of shoot- and root-respired CO₂ (Fig. IV.2). The rate of tracer increase in respired CO₂ of defoliated shoots proceeded much faster than in non-defoliated shoots (Figs. II.3 and IV.2). That is, the ratio of current photosynthate to stores as substrates for shoot respiration was higher in defoliated plants, indicating, that a large amount of respiratory stores were actually removed with the leaf blades. Conversely, root respiration relied to a larger extent and for longer time on pre-defoliation storage pools than the defoliated shoots, evidenced by the lower rate of tracer incorporation into respired CO₂.

Removing the majority of mature shoot tissue implies that the remaining shoot consists to a higher fraction of actively growing tissue. This also means that the growth respiration component gains relatively more importance in defoliated shoots. Root growth, on the other hand, was found to be strongly inhibited following defoliation (Davidson and

Milthorpe, 1966b; Richards, 1984), implying that maintenance respiration becomes a much larger fraction of total root respiration in plants subject to defoliation. Hence, the difference in the composition of shoot- and root-respired CO_2 with respect to current photosynthate and stores is in agreement with the notion, that stores are preferentially used for maintenance respiration, while growth respiration rather draws on current assimilate (Löttscher et al., 2004).

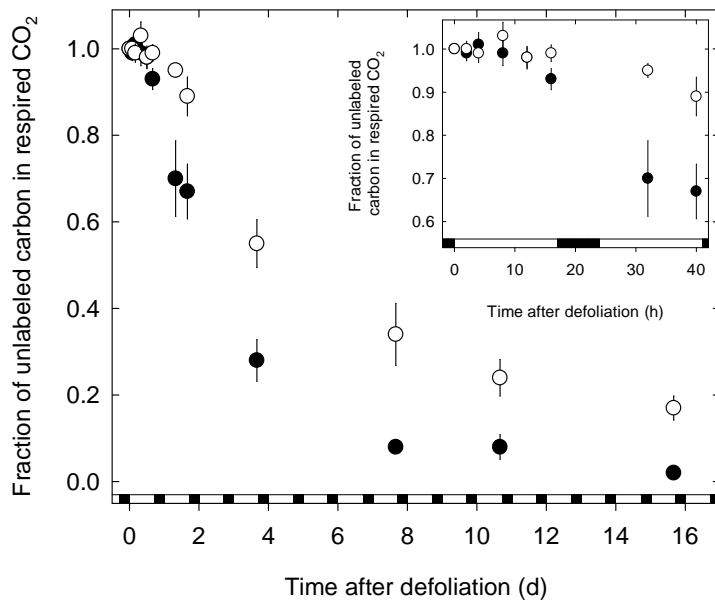


Figure IV.2: Evolution of the fraction of unlabeled carbon in CO_2 respired by shoots (black symbols) and roots (open symbols) of perennial ryegrass during labeling. Each value is the mean of two to six replicate plants ($\pm 1\text{SE}$). Inset expands the first 42 h. Plants were grown in the growth chamber system as described in chapters II and III, with a constant Temperature of 20°C , relative humidity of 85%, $360\ \mu\text{L L}^{-1} [\text{CO}_2]$ and a nitrogen supply of $7.5\ \text{mM}$ in the nutrient solution. Plants were grown in day/night-cycles with 16 h photoperiods (irradiance $425\ \mu\text{mol m}^{-2}\ \text{s}^{-1}$ PPFD at the top of the canopy) and 8 h dark periods, indicated by white and black horizontal bars. Shortly before the start of labeling at time 0 (*i.e.* the end of a dark period), when plants were 6-10 weeks old, the plants were subject to a severe defoliation, where all leaf blades were removed. Respiration measurements were carried out as described in chapters II and III. During the first light period following defoliation, virtually no tracer was detected in shoot- and root-respired CO_2 . Thereafter, the fraction of unlabeled carbon in shoot-respired CO_2 decreased rapidly, and after 8 d of defoliation, it approximated 0. The fraction of unlabeled carbon in root-respired CO_2 only started to decrease in the second light period after defoliation, and it occurred at a slower rate than observed for the shoot. Two weeks after defoliation, 20% of root-respired CO_2 was still unlabeled.

Under steady-state conditions (chapters II and III) plants maintained a constant root/shoot ratio throughout the experiment while defoliation caused (i) a dramatic change in the root/shoot ratio and (ii) presumably a change in the relative contribution of growth and maintenance respiration between organs. This, in turn, might have caused a change in the

allocation of stores towards root respiration, while current assimilates were preferentially respired in the shoot.

Two weeks after the severe disturbance of the system, the divergence in tracer content between shoot- and root-respired CO₂ tended to disappear, indicating that plants were restoring the state of a functional equilibrium between shoot and root resource acquisition again and the shoot to root transport rate of assimilates, a conclusion which is supported by the (nearly) complete recovery of specific shoot and root respiration rates to pre-defoliation values (data not shown).

Outlook

Respiration is the primary metabolic link between photosynthetic carbon gain and the subsequent use of assimilate in the sinks which require ATP, NAD(P)H and carbon skeletons. Thus, respiration operates in processes of growth (like the construction of new biomass), maintenance (like protein turnover) and in processes which may serve both functions (like phloem loading; Cannel and Thornley, 2000). Despite this complexity, the present study suggests that the respiratory carbon supply system of a whole intact plant may be reduced to only a few major components of carbon pools and fluxes. It was also shown that the respiratory supply systems of shoot and root are tightly linked. Furthermore, this tight plant-level integration held true for contrasting levels of nitrogen availability, although the system showed a remarkable flexibility concerning the regulation of the pools' contribution to respiration, especially concerning the participation of functionally distinct stores.

It is tempting to draw conclusions about the participation of a certain pool of the proposed model (Figs. II.4 and III.4) to processes associated with growth and maintenance requirements. And indeed, the system responses to nitrogen supply (chapter III), and to severe defoliation (chapter IV) suggest that the pools of current assimilation products rather served in growth respiration, whereas maintenance respiration drew more on old (storage) carbon. But although the growth-and-maintenance-respiration paradigm has been proved powerful in explaining plants' physiological responses to their environment, it must be kept in mind, that there is not a rigorous separation of respiratory processes as mentioned above. However, it is to be expected, that growth respiration processes predominate in growing meristems, while in mature tissue, the maintenance component constitutes the major part of respiratory activity. Thus, the application of the present approach at a smaller level of integration (like, for instance, studying the labeling kinetics of respiration in the growing *versus* the mature part of a leaf) would provide deeper insight into the carbon fluxes which resulted in the conceptual

model at the whole-plant level. Furthermore, studying the labeling kinetics of different metabolic components as putative substrates for respiration in physically and functionally distinct plant tissue (like growing blades or mature sheaths) seems a promising approach to move further towards the identification of respiratory substrate pools and fluxes, and thus, would help to better understand plant allocation patterns.

LITERATURE CITED

- Afzal M, Adams WA** (1992) Heterogeneity of soil mineral nitrogen in pasture grazed by cattle. *Soil Sci Soc Am J* **56**: 1160-1166
- Allard G, Nelson CJ** (1991) Photosynthate partitioning in basal zones of tall fescue leaf blades. *Plant Physiol* **95**: 663-668
- Amthor JS** (1989) *Respiration and crop productivity*. Springer Verlag, New York, US
- Amthor JS** (2000) The McCree-de Wit-Penning de Vries-Thornley respiration paradigms: 30 years later. *Ann Bot* **86**: 1-20
- ap Rees T** (1980) Assessment of the contributions of metabolic pathways to plant respiration. In DD Davies, ed, *The Biochemistry of Plants: A Comprehensive Treatise*, Vol. 2. Academic Press, San Diego, US, pp 1-29
- Atkins GL** (1969) *Multicompartment models in biological systems*. Methuen & Co. LTD, London, UK
- Avice JC, Ourry A, Lemaire G, Boucoud J** (1996) Nitrogen and carbon flows estimated by ¹⁵N and ¹³C pulse-chase labeling during regrowth of alfalfa. *Plant Physiol* **112**: 281-290
- Barbour MM, McDowell NG, Tcherkez G, Bickford CP, Hanson DT** (2007) A new measurement technique reveals rapid post-illumination changes in the carbon isotope composition of leaf-respired CO₂. *Plant Cell Environ* **30**: 469-482
- Bell CJ, Incoll LD** (1982) Translocation from the flag leaf of winter wheat in the field. *J Exp Bot* **33**: 896-909
- Benson AA** (2002) Paving the path. *Annu Rev Plant Biol* **53**: 1-25
- Bloom AJ, Caldwell RM, Finazzo J, Warner RL, Weissbart J** (1989) Oxygen and carbon dioxide fluxes from barley shoots depend on nitrate assimilation. *Plant Physiol* **91**: 352-356
- Bloom AJ, Sukrapanna SS, Warner RL** (1992) Root respiration associated with ammonium and nitrate absorption and assimilation by barley. *Plant Physiol* **99**: 1294-1301
- Bogaert N, Salomez J, Vermoesen A, Hofman G, Van Cleemput O, Van Meirvenne M** (2000) Within field variability of mineral nitrogen in grassland. *Biol Fertil Soils* **32**: 186-193
- Borland AM, Farrar JF** (1988) Compartmentation and fluxes of carbon in leaf blades and leaf sheaths of *Poa annua* L. and *Poa x jemtlandica* (Almq.) Richt. *Plant Cell Environ* **11**: 535-543
- Bowling DR, McDowell NG, Bond BJ, Law BE, Ehleringer JR** (2002) ¹³C content of ecosystem respiration is linked to precipitation and vapor pressure deficit. *Oecologia* **131**: 113-124
- Brouquisse R, James F, Raymond P, Pradet A** (1991) Study of glucose starvation in excised maize root tips. *Plant Physiol* **96**: 619-626
- Buchmann N, Ehleringer JR** (1998) CO₂ concentration profiles, and carbon and oxygen isotopes in C-3 and C-4 crop canopies. *Agric For Meteorol* **89**: 45-58
- Bürkle L, Hibberd JM, Quick WP, Kühn C, Hirner B, Frommer WB** (1998) The H⁺-sucrose cotransporter NtSUT1 is essential for sugar export from tobacco leaves. *Plant Physiol* **118**: 59-68
- Cannell MGR, Thornley JHM** (2000) Modelling the components of plant respiration: some guiding principles. *Ann Bot* **85**: 45-54
- Calvin M, Bassham JA** (1962) *The photosynthesis of carbon compounds*. WA Benjamin, New York, US
- Carbone MS, Trumbore SE** (2007) Contribution of new photosynthetic assimilates to respiration by perennial grasses and shrubs: residence times and allocation patterns. *New Phytol* **176**: 124-135

- Chapin FS, Schulze ED, Mooney HA** (1990) The ecology and economics of storage in plants. *Annu Rev Ecol Syst* **21**: 423-447
- Davidson JL, Milthorpe FL** (1966a) Leaf growth in *Dactylis glomerata* following defoliation. *Ann Bot* **30**: 173-184
- Davidson JL, Milthorpe FL** (1966b) The effect of defoliation on the carbon balance in *Dactylis glomerata*. *Ann Bot* **30**: 185-198
- Deléens E, Pavlidès D, Queiroz O** (1983) Application du tracage isotopique naturel per le ^{13}C à la mesure du renouvellement de la matière foliaire chez le plantes en C_3 . *Physiol Vég* **21**: 723-729
- Dewar RC, Medlyn BE, McMurtrie RE** (1998) A mechanistic analysis of light and carbon use efficiencies. *Plant Cell Environ* **21**: 573-588
- De Visser R, Vianden H, Schnyder H** (1997) Kinetics and relative significance of remobilized and current C and N incorporation in leaf and root growth zones of *Lolium perenne* after defoliation: assessment by ^{13}C and ^{15}N steady-state labelling. *Plant Cell Environ* **20**: 37-46
- Dieuaide-Noubhani M, Canioni P, Raymond P** (1997) Sugar-starvation-induced changes of carbon metabolism in excised maize root tips. *Plant Physiol* **115**: 1505-1513
- Dilkes NB, Jones DL, Farrar J** (2004) Temporal dynamics of carbon partitioning and rhizodeposition in wheat. *Plant Physiol* **134**: 706-715
- Dungey NO, Davies DD** (1982) Protein turnover in the attached leaves of non-stressed and stressed barley seedlings. *Planta* **154**: 435-440
- Ekblad A, Högberg P** (2001) Natural abundance of ^{13}C in CO_2 respired from forest soils reveals speed of link between tree photosynthesis and root respiration. *Oecologia* **127**: 305-308
- Evans JR** (1983) Nitrogen and photosynthesis in the flag leaf of wheat (*Triticum aestivum* L.). *Plant Physiol* **72**: 297-302
- Farquhar GD, Richards RA** (1984) Isotopic composition of plant carbon correlates with water-use efficiency of wheat genotypes. *Aust J Plant Physiol* **11**: 539-552
- Farquhar GD, Ehleringer JR, Hubick KT** (1989) Carbon isotope discrimination and photosynthesis. *Ann Rev Plant Physiol Plant Mol Biol* **40**: 503-537.
- Farrar JF** (1980) Allocation of carbon to growth, storage and respiration in the vegetative barley plant. *Plant Cell Environ* **3**: 97-105
- Farrar JF** (1985) The respiratory source of CO_2 . *Plant Cell Environ* **8**: 427-438
- Farrar JF** (1989) Fluxes and turnover of sucrose and fructans in healthy and diseased plants. *J Plant Physiol* **134**: 137-140
- Farrar JF** (1990) The Carbon balance of fast-growing and slow-growing species. In H Lambers, ML Cambridge, H Konings, TL Pons, eds, Causes and consequences of variation in growth rate and productivity of higher plants. SPB Academic Publishing, The Hague, The Netherlands, pp 241-256
- Farrar SC, Farrar JF** (1986) Compartmentation and fluxes of sucrose in intact leaf blades of barley. *New Phytol* **103**: 645-657
- Fernie AR, Carrari F, Sweetlove LJ** (2004) Respiratory metabolism: glycolysis, the TCA cycle and mitochondrial electron transport. *Curr Opin Plant Biol* **7**: 254-261
- Flanagan LB, Brooks JR, Varney GT, Berry SC, Ehleringer JR** (1996) Carbon isotope discrimination during photosynthesis and the isotope ratio of respired CO_2 in boreal forest ecosystems. *Global Biogeochem Cycles* **10**: 629-640
- Geiger DR, Swanson CA** (1965) Evaluation of selected parameters in a sugar beet translocation system. *Plant Physiol* **40**: 942-947
- Geiger DR, Saunders MA, Cataldo DA** (1969) Translocation and accumulation of translocate in the sugar beet petiole. *Plant Physiol* **44**: 1657-1665

- Geiger DR, Ploeger BJ, Fox TC, Fondy BR** (1983) Sources of sucrose translocated from illuminated sugar beet source leaves. *Plant Physiol* **72**: 964-970
- Geiger DR, Shieh WJ** (1988) Analysing partitioning of recently fixed and of reserve carbon in reproductive *Phaseolus vulgaris* L. plants. *Plant Cell Environ* **11**: 777-783
- Ghashghaie J, Badeck FW, Lanigan G, Nogués S, Tcherkez G, Deléens E, Cornic G, Griffiths H** (2003) Carbon isotope fractionation during dark respiration and photorespiration in C₃ plants. *Phytochem Rev* **2**: 145-161
- Gibon Y, Bläsing OE, Palacios-Rojas N, Pankovic D, Hendriks JHM, Fisahn J, Höhne M, Günther M, Stitt M** (2004) Adjustment of diurnal starch turnover to short days: depletion of sugar during the night leads to a temporary inhibition of carbohydrate utilization, accumulation of sugars and post-translational activation of ADP-glucose pyrophosphorylase in the following light period. *Plant J* **39**: 847-862
- Gifford RM** (2003) Plant respiration in productivity models: conceptualisation, representation and issues for global terrestrial carbon-cycle research. *Funct Plant Biol* **30**: 171-186
- Gleixner G, Danier HJ, Werner RA, Schmidt HL** (1993) Correlations between the ¹³C content of primary and secondary plant products in different cell compartments and that in decomposing basidiomycetes. *Plant Physiol* **102**: 1287-1290
- Hanba YT, Mori S, Lei TT, Koike T, Wada E** (1997) Variations in leaf $\delta^{13}\text{C}$ along a vertical profile of irradiance in a temperate Japanese forest. *Oecologia* **110**: 253-261
- Hansen AP, Yoneyama T, Kouchi H** (1992) Short-term nitrate effects on hydroponically-grown soybean cv. Bragg and its supernodulating mutant. II. Distribution and respiration of recently-fixed ¹³C-labelled photosynthate. *J Exp Bot* **43**: 9-14
- Heber U, Willenbrink J** (1964) Sites of synthesis and transport of photosynthetic products within the leaf cell. *Biochim Biophys Acta* **82**: 313-324
- Heldt HW** (2005) *Plant biochemistry*. Elsevier Academic Press, San Diego, US
- Hikosaka K, Hanba YT, Hirose T, Terashima I** (1998) Photosynthetic nitrogen-use efficiency in leaves of woody and herbaceous species. *Funct Ecol* **12**: 896-905
- van Iersel MW** (2003) Carbon use efficiency depends on growth respiration, maintenance respiration, and relative growth rate. A case study with lettuce. *Plant Cell Environ* **26**: 1441-1449
- Imsande J, Touraine B** (1994) N demand and the regulation of nitrate uptake. *Plant Physiol* **105**: 3-7
- Jacquez JA** (1996) *Compartmental Analysis in Biology and Medicine*, 3rd Edition. Biomedware, Ann Arbor, US
- Johnson IR** (1990) Plant respiration in relation to growth, maintenance, ion uptake and nitrogen assimilation. *Plant Cell Environ* **13**: 319-328
- Johnson D, Leake JR, Ostle N, Ineson P, Read DJ** (2002) *In situ* ¹³CO₂ pulse-labelling of upland grassland demonstrates a rapid pathway of carbon flux from arbuscular mycorrhizal mycelia to the soil. *New Phytol* **153**: 327-334
- Klumpp K, Schäufele R, Lötscher M, Lattanzi FA, Feneis W, Schnyder H** (2005) C-isotope composition of CO₂ respired by shoots and roots: fractionation during dark respiration? *Plant Cell Environ* **28**: 241-250
- Knohl A, Werner RA, Brand WA, Buchmann N** (2005) Short-term variations in $\delta^{13}\text{C}$ of ecosystem respiration reveals link between assimilation and respiration in a deciduous forest. *Oecologia* **142**: 70-82
- Kouchi H, Yoneyama T** (1984) Dynamics of carbon photosynthetically assimilated in nodulated soya bean plants under steady-state conditions. 1. Development and application of ¹³CO₂ assimilation system at a constant ¹³C abundance. *Ann Bot* **53**: 875-882

- Kouchi H, Nakaji K, Yoneyama T, Ishizuka J** (1985) Dynamics of carbon photosynthetically assimilated in nodulated soya bean plants under steady-state conditions. 3. Time-course study on ^{13}C incorporation into soluble metabolites and respiratory evolution of $^{13}\text{CO}_2$ from roots and nodules. *Ann Bot* **56**: 333-346
- Kouchi H, Akao S, Yoneyama T** (1986) Respiratory utilization of ^{13}C -labelled photosynthate in nodulated root systems of soybean plants. *J Exp Bot* **37**: 985-993
- Lattanzi FA, Schnyder H, Thornton B** (2005) The sources of carbon and nitrogen supplying leaf growth. Assessment of the role of stores with compartmental models. *Plant Physiol* **137**: 383-395
- Lawlor DW, Kontturi M, Young AT** (1989) Photosynthesis by flag leaves of wheat in relation to protein, ribulose biphosphate carboxylase activity and nitrogen supply. *J Exp Bot* **40**: 43-52
- Lea PJ, Ireland RJ** (1999) Nitrogen metabolism in higher plants. In BK Singh, ed, *Plant amino acids*. Marcel Dekker, New York, US, pp 1-47
- Leport L, Kandlbinder A, Baur B, Kaiser WM** (1996) Diurnal modulation of phosphoenolpyruvate carboxylation in pea leaves and roots as related to tissue malate concentrations and to the nitrogen source. *Planta* **198**: 495-501
- Lötscher M, Klumpp K, Schnyder H** (2004) Growth and maintenance respiration for individual plants in hierarchically structured canopies of *Medicago sativa* and *Helianthus annuus*: the contribution of current and old assimilates. *New Phytol* **164**: 305-316
- Lötscher M, Gayler S** (2005) Contribution of current photosynthates to root respiration of non-nodulated *Medicago sativa*: effects of light and nitrogen supply. *Plant Biol* **7**: 601-610
- Makino A, Osmond B** (1991) Effects of nitrogen nutrition on nitrogen partitioning between chloroplasts and mitochondria in pea and wheat. *Plant Physiol* **96**: 355-362
- Matyssek R, Schnyder H, Elstner EF, Munch JC, Pretzsch H, Sandermann H** (2002) Growth and parasite defence in plants; the balance between resource sequestration and retention: In lieu of a guest editorial. *Plant Biol* **4**: 133-136
- McDermitt DK, Loomis RS** (1981) Elemental composition of biomass and its relation to energy content, growth efficiency, and growth yield. *Ann Bot* **48**: 275-290
- Mooney HA, Fichtner K, Schulze ED** (1995) Growth, photosynthesis and storage of carbohydrates and nitrogen in phaseolus lunatus in relation to resource availability. *Oecologia* **104**: 17-23
- Moorby J, Jarman PD** (1975) The use of compartmental analysis in the study of the movement of carbon through leaves. *Planta* **122**: 155-168
- Morvan-Bertrand A, Boucaud J, Prud'homme MP** (1999) Influence of initial levels of carbohydrates, fructans, nitrogen, and soluble proteins on regrowth of *Lolium perenne* L. cv Bravo following defoliation. *J Exp Bot* **50**: 1817-1826
- Nogués S, Tcherkez G, Cornic G, Ghashghaie J** (2004) Respiratory carbon metabolism following illumination in intact French bean leaves using $^{13}\text{C}/^{12}\text{C}$ isotope labeling. *Plant Physiol* **136**: 3245-3254
- Park R, Epstein S** (1961) Metabolic fractionation of C^{13} & C^{12} in plants. *Plant Physiol* **36**: 133-138
- Penning de Vries FWT, Brunsting AHM, Van Laar HH** (1974) Products, requirements and efficiency of biosynthesis: a quantitative approach. *J Theor Biol* **45**: 339-377
- Penning de Vries FWT** (1975) The cost of maintenance processes in plant cells. *Ann Bot* **39**: 77-92
- Plaxton WC, Podestá FE** (2006) The functional organization and control of plant respiration. *Crit Rev Plant Sci* **25**: 159-198

- Pollock CJ, Cairns AJ** (1991) Fructan metabolism in grasses and cereals. *Ann Rev Plant Physiol Plant Mol Biol* **42**: 77-101
- Poorter H, Nagel O** (2000) The role of biomass allocation in the growth response of plants to different levels of light, CO₂, nutrients and water: a quantitative review. *Aust J Plant Physiol* **27**: 595-607
- Prosser J, Farrar JF** (1981) A compartmental model of carbon allocation in the vegetative barley plant. *Plant Cell Environ* **4**: 303-307
- R Development Core Team** (2007) R: A language and environment for statistical computing. R foundation for statistical computing, Vienna, Austria. URL: <http://www.R-project.org>
- Ratcliffe RG, Shachar-Hill Y** (2006) Measuring multiple fluxes through plant metabolic networks. *Plant J* **45**: 490-511
- Reich PB, Tjoelker MG, Machado JL, Oleksyn J** (2006) Universal scaling of respiratory metabolism, size and nitrogen in plants. *Nature* **439**: 457-461
- Rescigno A** (2001) The rise and fall of compartmental analysis. *Pharmacol Res* **44**: 337 - 342
- Richards JH** (1984) Root growth response to defoliation in two Agropyron bunchgrasses: field observations with an improved root periscope. *Oecologia* **64**: 21-25
- Robson MJ, Deacon MJ** (1978) Nitrogen deficiency in small closed communities of S24 ryegrass. II. Changes in the weight and chemical composition of single leaves during their growth and death. *Ann Bot* **42**: 1199-1213
- Rocher JP, Prioul JL** (1987) Compartmental analysis of assimilate export in a mature maize leaf. *Plant Physiol Biochem* **25**: 531-540
- Ruben S, Kamen MD** (1941) Long-lived radioactive carbon: C¹⁴. *Phys Rev* **59**: 349-354
- Ryle GJA, Cobby JM, Powell CE** (1976) Synthetic and maintenance respiratory losses of ¹⁴CO₂ in unculm barley and maize. *Ann Bot* **40**: 571-586
- Schimel DS** (1995) Terrestrial ecosystems and the carbon-cycle. *Glob Change Biol* **1**: 77-91
- Schnyder H, Nelson CJ** (1987) Growth rates and carbohydrate fluxes within the elongation zone of tall fescue leaf blades. *Plant Physiol* **85**: 548-553
- Schnyder H** (1992) Long-term steady-state labelling of wheat plants by use of natural ¹³CO₂/¹²CO₂ mixtures in an open, rapidly turned over system. *Planta* **187**: 128-135
- Schnyder H, de Visser R** (1999) Fluxes of reserve-derived and currently assimilated carbon and nitrogen in perennial ryegrass recovering from defoliation. The regrowing tiller and its component functionally distinct zones. *Plant Physiol* **119**: 1423-1435
- Schnyder H, Schäufele R, Lötscher M, Gebbing T** (2003) Disentangling CO₂ fluxes: direct measurements of mesocosm-scale natural abundance ¹³CO₂/¹²CO₂ gas exchange, ¹³C discrimination, and labelling of CO₂ exchange flux components in controlled environments. *Plant Cell Environ* **26**: 1863-1874
- Schnyder H, Schwertl M, Auerswald K, Schäufele R** (2006) Hair of grazing cattle provides an integrated measure of the effects of site conditions and interannual weather variability on δ¹³C of temperate humid grassland. *Glob Change Biol* **12**: 1-15
- Simpson E, Cooke RJ, Davies DD** (1981) Measurement of protein degradation in leaves of *Zea mays* using [³H]acetic anhydride and tritiated water. *Plant Physiol* **67**: 1214-1219
- Smith AM, Stitt M** (2007) Coordination of carbon supply and plant growth. *Plant Cell Environ* **30**: 1126-1149
- Sparks JP, Ehleringer JR** (1997) Leaf carbon isotope discrimination and nitrogen content for riparian trees along elevational transects. *Oecologia* **109**: 362-367
- Stitt M, Müller C, Matt P, Gibon Y, Carillo P, Morcuende R, Scheible WR, Krapp A** (2002) Steps towards an integrated view of nitrogen metabolism. *J Exp Bot* **53**: 959-970
- Sullivan JT, Sprague VG** (1943) Composition of the roots and stubble of perennial ryegrass following partial defoliation. *Plant Physiol* **18**: 656-670

- Suzuki M** (1971) Semi-automatic analysis of the total available carbohydrates in alfalfa roots. *Can J Plant Sci* **51**: 184-185
- Tcherkez G, Nogués S, Bleton J, Cornic G, Badeck F, Ghashghaie J** (2003) Metabolic origin of carbon isotope composition of leaf dark-respired CO₂ in french bean. *Plant Physiol* **131**: 237-244
- Thome U, Kühbauch W** (1985) Change in the carbohydrate pattern in the cell content of wheat stems during grain-filling. *J Agronomy & Crop Science* **155**: 253-260
- Trumbore S** (2006) Carbon respired by terrestrial ecosystems – recent progress and challenges. *Glob Change Biol* **11**: 1-13
- Vijn I, Smeekens S** (1999) Fructan: more than a reserve carbohydrate? *Plant Physiol* **120**: 351-359
- Windt CW, Vergeldt FJ, de Jager PA, Van As H** (2006) MRI of long-distance water transport: a comparison of the phloem and xylem flow characteristics and dynamics in poplar, castor bean, tomato and tobacco. *Plant Cell Environ* **29**: 1715-1729
- Winzeler M, Dubois D, Nösberger J** (1990) Absence of fructan degradation during fructan accumulation in wheat stems. *J Plant Physiol* **136**: 324-329

Lebenslauf

Name: Christoph Andreas Lehmeier
Geb. am: 9. Juli 1972
Geburtsort: Neumarkt/Oberpfalz
Staatsangehörigkeit: deutsch

Schulische Ausbildung

1978 – 1982 Grundschule Wolfstein, Neumarkt
1982 – 1991 Willibald-Gluck-Gymnasium, Neumarkt

Berufliche Ausbildung

1991 – 1994 Lehre zum Modellbauer/Handwerk
Modell- und Formenbau Holzammer GmbH, Sengenthal

Berufliche Tätigkeit

1994 – 1997 Modell- und Formenbau Holzammer GmbH, Sengenthal

Universitäre Ausbildung

1997 – 2003 Studium der Agrarwissenschaften
Technische Universität München, Weihenstephan
Auslandssemester an der Università di Bologna/Italien
12/2003 Abschluss zum Diplom-Agraringenieur

Akademische Beschäftigung

1/2004 – 6/2004 Wissenschaftlicher Mitarbeiter am Lehrstuhl für Grünlandlehre
Technische Universität München, Weihenstephan
6/2004 – 9/2008 Doktorand am Lehrstuhl für Grünlandlehre